

2010

# A Nonlinear ODE Model of Tumor Growth and Effect of Immunotherapy and Chemotherapy Treatment in Colorectal Cancer

Hannah P. Savage  
*Harvey Mudd College*

---

## Recommended Citation

Savage, Hannah P., "A Nonlinear ODE Model of Tumor Growth and Effect of Immunotherapy and Chemotherapy Treatment in Colorectal Cancer" (2010). *HMC Senior Theses*. 20.  
[https://scholarship.claremont.edu/hmc\\_theses/20](https://scholarship.claremont.edu/hmc_theses/20)

This Open Access Senior Thesis is brought to you for free and open access by the HMC Student Scholarship at Scholarship @ Claremont. It has been accepted for inclusion in HMC Senior Theses by an authorized administrator of Scholarship @ Claremont. For more information, please contact [scholarship@cuc.claremont.edu](mailto:scholarship@cuc.claremont.edu).



A Nonlinear ODE Model of Tumor Growth  
and Effect of Immunotherapy and  
Chemotherapy Treatment in Colorectal Cancer

**Hannah Savage**

Lisette de Pillis, Advisor

Ami Radunskaya, Reader

May, 2010

**HARVEY MUDD**  
COLLEGE

Department of Mathematics

Copyright © 2010 Hannah Savage.

The author grants Harvey Mudd College the nonexclusive right to make this work available for noncommercial, educational purposes, provided that this copyright statement appears on the reproduced materials and notice is given that the copying is by permission of the author. To disseminate otherwise or to republish requires written permission from the author.

# Abstract

Colorectal cancer will kill approximately 50,000 people in the United States this year (ACS, 2008). Current treatment options, including surgery, chemotherapy, and radiation, are often able to force the cancer into remission, but better treatments are needed to help those who don't respond to current treatments. A new and promising treatment option, monoclonal-antibody therapy, has the potential to help reduce the deaths caused by colorectal cancer, but most monoclonal-antibody drugs are currently still in trial phases, and the variations in the dosing schedule of those currently approved for use have not been heavily explored. We have modified a non-linear ODE tumor/treatment model by de Pillis and colleagues (2009) to include monoclonal antibody treatments. Parameter values have been modified for colorectal cancer, with irinotecan as the chemotherapy agent and the two monoclonal antibodies cetuximab, which is FDA approved, and panitumumab, which is still undergoing clinical trials. We have run Matlab simulations of current treatment options, and have found new dosing schedules which, in our simulations, reduce tumor size more effectively than the current schedules. Equilibria of the system and its sensitivity to parameters have also been examined.



# Contents

<b>Abstract</b>	<b>iii</b>
<b>Acknowledgments</b>	<b>xi</b>
<b>1 Introduction</b>	<b>1</b>
<b>2 Biology Background</b>	<b>3</b>
2.1 The Healthy Colon . . . . .	3
2.2 Overview of the Immune System . . . . .	3
2.3 Colon Cancer and Treatments . . . . .	7
<b>3 Prior Mathematical Work</b>	<b>11</b>
3.1 ODE Tumor Models . . . . .	11
3.2 PDE Tumor Models . . . . .	12
<b>4 Equations</b>	<b>15</b>
4.1 System of Equations . . . . .	16
4.2 Justifications of New Terms . . . . .	17
<b>5 Parameters</b>	<b>21</b>
5.1 Initial Conditions . . . . .	21
5.2 Equation 4.1 Parameters . . . . .	25
5.3 Equation 4.2 Parameters . . . . .	29
5.4 Equation 4.3 Parameters . . . . .	31
5.5 Equation 4.4 Parameters . . . . .	33
5.6 Equation 4.5 Parameters . . . . .	34
5.7 Equation 4.6 Parameters . . . . .	34
5.8 Equation 4.7 Parameters . . . . .	35
5.9 Treatments . . . . .	37

<b>6</b>	<b>Results and Analysis</b>	<b>41</b>
6.1	Current Monotherapies . . . . .	42
6.2	Current Combination Treatments . . . . .	42
6.3	Tumor Growth With Experimental Treatments . . . . .	48
6.4	Sensitivity to Parameters . . . . .	51
<b>7</b>	<b>Discussion</b>	<b>55</b>
<b>A</b>	<b>Biology Glossary</b>	<b>59</b>
<b>B</b>	<b>Reference Tables</b>	<b>63</b>
B.1	Equation Term Descriptions . . . . .	63
B.2	Parameter Descriptions . . . . .	65
B.3	Parameter Values . . . . .	67
	<b>Bibliography</b>	<b>69</b>

# List of Figures

2.1	Normal and cancerous colon crypts . . . . .	4
2.2	Types of blood cells . . . . .	5
4.1	Possible MAB pathways . . . . .	17
5.1	Stable Equilibria. . . . .	22
5.2	Small and large initial tumors. . . . .	24
5.3	The probability density function of $x$ and $y$ . . . . .	27
5.4	Activated CD8 <sup>+</sup> T-cell treatment schedule. . . . .	38
5.5	Irinotecan dosing schedule. . . . .	38
5.6	Monoclonal antibody dosing schedules. . . . .	40
6.1	Irinotecan Monotherapies. . . . .	43
6.2	Cetuximab Monotherapies. . . . .	43
6.3	Panitumumab Monotherapies. . . . .	44
6.4	Combination Therapy: Weak tumor response. . . . .	45
6.5	Combination Therapy: Mixed tumor response. . . . .	45
6.6	Combination Therapy: Strong tumor response. . . . .	46
6.7	Combination Therapy: Strong tumor response, low $l/s$ . . . . .	46
6.8	Experimental: Cetuximab Offset. . . . .	49
6.9	Experimental: Panitumumab Offset. . . . .	49
6.10	Experimental: High dose irinotecan and cetuximab. . . . .	49
6.11	Experimental: High dose irinotecan and panitumumab. . . . .	49
6.12	Parameter sensitivity with 5% change. . . . .	52
6.13	Sensitivity to cetuximab parameters. . . . .	52
6.14	Sensitivity to panitumumab parameters. . . . .	53
6.15	Sensitivity to irinotecan parameters. . . . .	53



# List of Tables

6.1	Response Rates to Common Treatments . . . . .	47
6.2	Response Rates to Experimental Treatments . . . . .	50
B.1	Equation Descriptions . . . . .	63
B.2	Parameter Descriptions . . . . .	65
B.3	Parameter Values. . . . .	67



# Acknowledgments

I would like to thank Professor Lisette de Pillis for her guidance and support throughout this semester. I would also like to thank my second reader, Professor Ami Radunskaya, Claire Connelly for her  $\text{\LaTeX}$  help and advice, and the Harvey Mudd College Department of Mathematics.



# Chapter 1

## Introduction

Cancer is one of the leading causes of death in the United States, behind only heart disease (ACS, 2008). According to the American Cancer Society, colorectal cancer accounts for approximately 10 percent of cancer cases in the United States, and approximately 9 percent of cancer-related deaths (ACS, 2008). Colorectal cancer is mainly a disease of the elderly, with a median age at diagnosis of 71 years (Goldberg and Carrato, 2008). Although colorectal cancer incidence rates have declined over the last 10 years, it is still a significant cause of death in the United States (ACS, 2008). A new treatment option, the use of monoclonal antibody drugs, has recently been explored as a possible approach to controlling colorectal cancer, but there are still many unanswered questions about the effectiveness of monoclonal antibodies and how they should be used. The goal of this work is to contribute to the understanding of how best to use monoclonal antibodies in the treatment of colorectal cancer. We have built a system of nonlinear ordinary differential equations (ODEs) that model the growth of a colorectal tumor and its interactions with the host's immune system. Using this model, we consider three different types of treatment. We will then run simulations and examine possible treatment regimens.

Chapter 2 gives an overview of the anatomy of the colon and rectum, the relevant features of the immune system, the growth of a colorectal tumor, and some of the current treatment options. Chapter 3 gives an overview of the previous work done to mathematically model colorectal tumors and treatments. Chapter 4 describes the system of equations, and Chapter 5 describes the parameters used in the equations. Chapter 6 presents our results and analysis of the model, and Chapter 7 is a discussion of the significance of our results and possible future directions.



## Chapter 2

# Biology Background

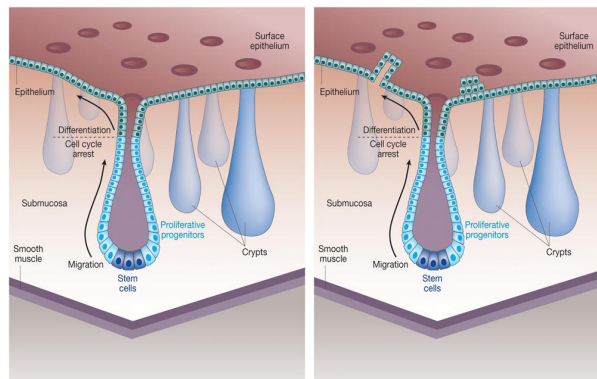
To understand why the terms in our equations have been added and how the parameters have been derived, it is first necessary to understand how the human immune system functions and how it interacts with a growing tumor.

### 2.1 The Healthy Colon

The colon and rectum are found at the end of our gastrointestinal tract, which is responsible for digesting food and absorbing nutrients. The surface of our colon is covered by a single layer of epithelial cells and is lined with small pits called “crypts” (Sompayrac, 2004). The cells in our colon and rectum have a lifetime of less than one week, and so are continually replaced by the proliferation of stem cells that can reproduce indefinitely (Sompayrac, 2004). These stem cells are found at the bottom of the crypts, and as they create new epithelial cells, the old cells are pushed to the surface and removed (Figure 2.1(a)) (Sompayrac, 2004). In a healthy colon, stem-cell proliferation is carefully controlled, and just enough new epithelial cells are produced to replace those that have died (Sompayrac, 2004). However, if mutations occur in the growth-control system of an epithelial cell, this careful control can be lost, and a tumor is formed (Figure 2.1(b)).

### 2.2 Overview of the Immune System

This section will briefly explain the role of the cells and protein messengers in the immune system relevant to this model for colorectal cancer. It will



(a) Normal crypt.

(b) Cancerous crypt.

Figure 2.1: A normal crypt in the colon, and a crypt that has developed mutations and become cancerous (Reya and Clevers, 2005).

look at two parts of the immune system: the *innate immune system*, which responds quickly to invaders, but with a nonspecific and less effective response, and the *adaptive immune system*, which responds more slowly but is targeted at a specific invader. Information on other parts of the immune system, as well as a summary of the parts of the immune system discussed here, can be found in Appendix A. Unless otherwise noted, this information is from Lauren Sompayrac's *How the Immune System Works* (2008).

### 2.2.1 Innate Immune System

The innate immune system responds to invaders as soon as they enter the body. It uses three main response pathways: *the complement system*, *professional phagocytes*, and *natural killer cells*. The complement system is composed of about 20 proteins that, when activated, can destroy invaders through a process called *complement-dependent cytotoxicity* (CDC). The complement system can be activated in multiple ways, one of which is activation by antibodies, which we will explain as part of our discussion of the adaptive immune system in Section 2.2.2.

When blood cells mature, they can become either hemoglobin-carrying "red" blood cells, or they can become the cells of our immune system, the non hemoglobin-carrying "white" blood cells, or *leukocytes* (Figure 2.2). The professional phagocytes are made up of two different kinds of leukocytes, and are responsible for engulfing invaders and destroying them.

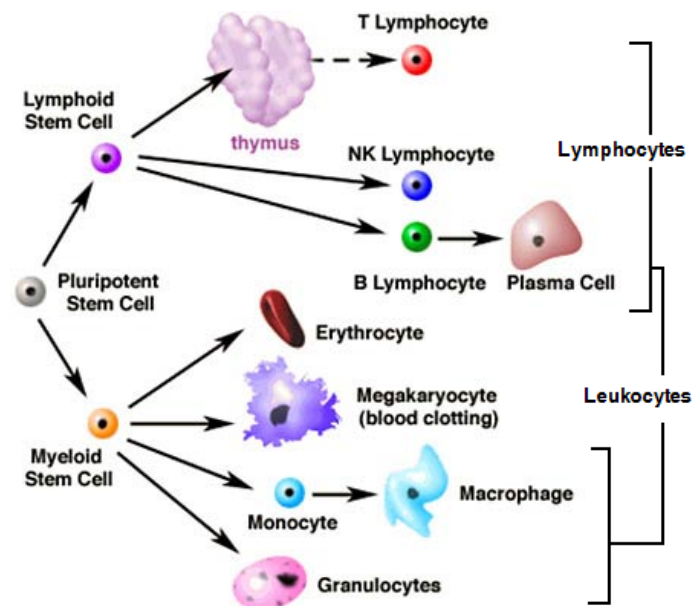


Figure 2.2: Types of blood cells (Dharmananda, 2005).

### Natural Killer Cells

Natural killer cells (NK cells), another type of leukocyte, have multiple jobs. When they receive chemical signals called *cytokines* from other members of the innate immune system, they are responsible for producing more of these signals and passing them on to other cells. NK cells are also responsible for examining the proteins present on a cell and deciding whether or not that cell belongs to the host. NK cells look for a protein called *MHC I*, which displays short peptide sequences called *antigens* from the proteins contained in the cell. Most of our cells have many copies of MHC I on their surface, and these proteins inhibit NK cells. So, if an NK cell find a cell that does not display many MHC I proteins, it can induce *apoptosis*, causing the cell to commit suicide. However, NK cells need to be activated before they can search for invading cells. One way that they can be activated is with interleukin-2 (IL-2), a type of cytokine. Another method of NK cell activation relying on antibodies, called *antibody-dependent cellular cytotoxicity* (ADCC), will be explained as part of the discussion of the adaptive immune system in Section 2.2.2.

### 2.2.2 Adaptive Immune System

Once the innate immune system has been activated, the adaptive immune system begins making antibodies for the current invader. These antibodies are pieces of proteins which match the invader's, but not the host's, proteins, and tell leukocytes which cells to destroy. Antibodies have many jobs, including guiding macrophages and activating the complement cascade, but lymphocyte activation is their most important job. *Lymphocytes*, a type of leukocyte, are programmed to find invaders matching their antibodies, and to effectively kill them. Killer T-cells and NK cells are the two types of lymphocytes we will look at specifically in this model.

#### Killer T-Cells

Killer T-cells (or cytotoxic T cells, CTLs), part of the adaptive immune system, are responsible for finding invaders once the invaders have already entered a cell. Each CTL contains receptors which bind to a specific antigen that the body has already verified belongs to an invader. Once a CTL has been activated, the CTL's receptors search for a cell with its specific antigen. When the CTL finds its antigen, a protein on the surface of the CTL, called CD8+, binds to the antigen, an MHC I protein on the invader, and induces apoptosis. However, before a CTL can find invaders, it must wait for the innate immune system to detect invaders and send out interleukin-2, which activates the CTLs.

#### Natural Killer Cells and the Adaptive Immune System

NK cells can also interact with certain types of antibodies. Antibodies are small proteins that bind to foreign peptide sequences displayed by MHC I proteins, and, by also binding to other cells in our immune system, create a link between the two and allow for more effective killing. Some antibodies, specifically certain subclasses of the IgG antibodies, are able to bind to NK cells, making the NK cells more cytotoxic (more effective killers). These antibodies simultaneously activate the NK cells and direct them to their target. This process is called "antibody-dependent cellular cytotoxicity" (ADCC).

## 2.3 Colon Cancer and Treatments

Normal cells undergo carefully regulated cell division (*proliferation*). However, cells are mutated, this carefully controlled regulation can be lost. This section will describe what happens when colon cells proliferate, and how this problem can be treated. Unless otherwise noted, this information is from Lauren Sompayrac's *How Cancer Works* (2004).

### 2.3.1 Colon Cancer

When mutations occur, the normal control systems of cells can be damaged or lost. Mutations affecting the growth control systems happen frequently in the epithelial cells of the colon as we age, causing "fingers" of cells called *polyps* to grow out from the colon wall. New blood vessels develop within these polyps, allowing the cells to extend further outward. Polyps can be removed fairly easily and examined to see what mutations the cells have undergone. Most mutations that result in polyp formation only give the cell a small proliferation advantage, and these polyps are considered benign. However, approximately 1 percent of these polyps will become cancerous, and will have unregulated proliferation. Many will also have other mutations that destroy the cells' ability to divide correctly and check for errors during cell division, resulting in even more mutations. The cells from these cancerous polyps will break off into the blood stream, and then reattach themselves at another location in the body and begin proliferating again. When this happens, the tumor is said to have *metastasized*, and can no longer be removed by surgery alone.

### 2.3.2 Current Treatments

Surgery is often an effective treatment option for colorectal cancer. However, if the tumor has metastasized, or if the oncologist wants to ensure that all of the cancerous cells have been removed, other treatment options may also be used.

#### Chemotherapy

Chemotherapy involves the administration of chemicals into the blood that target cell division. Thus the cells in the body that normally have a high turnover rate (such as any cancerous cells present) are no longer able to reproduce. Chemotherapy drugs are now being used in conjunction with

other medications aimed at strengthening the response of the immune system (Gravalos et al., 2009; Siena et al., 2009; Martinelli et al., 2009; De Vita, Jr et al., 2000).

### Immunotherapy

Many cells in our body rely on epidermal growth factor (EGF) to help them decide when to proliferate. The binding of EGF to an epidermal growth-factor receptor (EGFR) triggers a signaling cascade in the cell that results in cell proliferation (Martinelli et al., 2009). Many tumors have a mutation that *upregulates*, or increases, the number of epithelial growth factor receptors (Gravalos et al., 2009; Siena et al., 2009; Martinelli et al., 2009; De Vita, Jr et al., 2000). Because so many cancerous cells have this mutation, these EGFRs have recently become the target of a new cancer treatment, monoclonal antibodies.

Monoclonal antibodies (MABs) are small antibodies that are manufactured to bind to specific proteins. Some monoclonal antibodies compete with EGF to bind to the *extracellular domain* of EGFR, the part of the receptor that protrudes from the cell, waiting for an EGF to bind. Monoclonal antibodies have a much higher affinity for EGFR than EGF does, and thus they are able to prevent EGFs from binding to EGFR and the proliferation signaling cascade from starting (Martinelli et al., 2009). When the cells with high numbers of EGFRs can no longer proliferate as quickly, the immune system has a better chance of killing them before they can multiply further.

Cetuximab and panitumumab, both monoclonal antibodies that target EGFR, are promising new treatments for colorectal cancer. Cetuximab, used with or without the chemotherapy medication irinotecan, has been shown to improve survival times and quality of life (Martinelli et al., 2009). Cetuximab is an IgG1 antibody, a subclass that is able to elicit ADCC from NK cells, thus increasing the NK cells' cytotoxicity (Martinelli et al., 2009). Panitumumab is a newer drug and has undergone fewer clinical trials. Panitumumab has been shown to decrease tumor growth rate, but the clinical trials have not yet been able to confirm that it increases overall survival time (Martinelli et al., 2009). Both cetuximab and panitumumab are able to activate the complement cascade of the innate immune system (De Vita, Jr et al., 2000). Both are also able to increase chemotherapy's toxicity to tumor cells, because the tumor cells are killed more easily and cannot replace their population as quickly when they are unable to reproduce (De Vita, Jr et al., 2000).

Currently, monoclonal-antibody treatments are very new and are mainly used in patients with metastatic cancer, particularly when no other treatment has worked (Martinelli et al., 2009). However, it is possible that with the positive results from current clinical trials, monoclonal antibodies may become a more significant part of colorectal-cancer treatment.



## Chapter 3

# Prior Mathematical Work

Many previous tumor models have been created, although very few look specifically at colorectal cancer, and none have been found in our research that model monoclonal antibodies. We will briefly present the models created by de Pillis and colleagues (2009; 2008; 2005), on which this work is based, and will then examine others models which may be a useful comparison and reference for our work.

### 3.1 ODE Tumor Models

Much of the work previously done on cancer modeling, particularly for colon cancer, has examined spatial growth, and so builds a system of partial differential equations (PDEs). We will be using ordinary differential equations (ODEs) in our model, and so will focus our description of previous work on models using ODE systems.

#### 3.1.1 Previous Versions of Our Model

The model presented here is developed from the work of de Pillis and colleagues, in which tumor-cell population, immune-cell populations, and drug concentrations are modeled with a series of nonlinear ODEs. This model also includes patient-specific parameters representing the strength of the patient's immune system. This model has been validated with published studies on mice and humans (de Pillis et al., 2005). It has successfully demonstrated the need for immunotherapy in addition to chemotherapy to prevent the tumor from growing again after drug therapies have been completed, and has studied the importance of the patient-specific parameters in

the effectiveness of immunotherapy treatment (de Pillis et al., 2009, 2008). This work adapts the model of de Pillis and colleagues to include terms for monoclonal-antibody treatment and adjusts the parameters to fit specifically with colorectal cancer.

### 3.1.2 Other ODE Models

Simpler ODE models have also been developed to describe the development of tumors (Gatenby and Vincent, 2003; Kuznetsov et al., 1994). These models are both used mainly to examine equilibrium points. Gatenby and Vincent (2003) track populations of tumor cells and normal cells. They show that with only chemotherapy, there is an unstable equilibrium point when the tumor cell population is zero, and a stable equilibrium point when the tumor cell population reaches the carrying capacity of the tissue. They concluded that with only chemotherapy, the growth rate of the tumor-cell population is always positive as long as the tumor-population is positive. Thus, according to Gatenby and Vincent's model, chemotherapy alone will not be enough to prevent the tumor from rebounding. This agrees with the conclusions of de Pillis and colleagues (2008).

Kuznetsov's team (1994) tracks populations of cytotoxic cells and tumor cells. Their model shows a theoretical value where the host's immune system will be able to keep the tumor-cell population under control indefinitely. However, Kuznetsov and colleagues acknowledge that as time progresses, some change will occur (e.g. a change in immune-system parameters or a new mutation in the tumor cells) that will cause tumor growth to cross the bifurcation border. They found that one of the most critical parameters was a value representing the rate at which cytotoxic cells were inactivated due to interactions with the tumor (Kuznetsov et al., 1994).

## 3.2 PDE Tumor Models

Ordinary differential equations are, computationally, much easier to work with than partial differential equations. However, the use of ODEs in this work requires the simplifying assumption of a cell count to represent a three-dimensional tumor, and assumes that every cell is identical, regardless of its location in the tumor. Thus it is important to verify that this simplification does not adversely affect the accuracy of the model. For this, we find the work of Johnston and colleagues (2007) to be useful.

Johnston's team (2007) consider two different approaches to the modeling of cells in a colonic crypt. They first consider a compartmental approach, which tracks the locations and ages of stem cells; transit cells, which move up the wall of the crypt to the surface; and differentiated cells. Each of these populations, located in different parts of the colonic crypt, has different characteristics. As the cells mature they move through the different compartments, corresponding to a physical movement of the crypt walls towards the surface of the colon. In this model, Johnston's team sets a different cell-cycle length for each of the cell populations, so that the cells can divide and mature further at different rates, depending on where they are located in the crypt. With this first model, they tracked the cell cycles of each cell, which provided information on how quickly the cell was moving between compartments, and thus could be used to find an overall growth rate.

However, this approach resulted in equations which were very difficult to work with. So, the authors also developed a continuous approximation for their equations by integrating over all cell ages. The resulting ODE system still considers the cell populations to be separate, but movement between cell populations is just considered to be a rate instead of taking into account the discrete movement of cells resulting from different cell cycle lengths. They found that this continuous model provided a good approximation for the growth rate found by the age-differentiated model, for a sufficiently large time scale.



## Chapter 4

# Equations

In this update of the model presented by de Pillis and colleagues (2009), we will include a new treatment option, monoclonal antibodies, and will remove the interleukin treatment option. IL-2 treatments are not effective against colorectal cancer (Rosenberg, 1988), and thus are not used here. We will also modify parameters to be specific to colorectal cancer and the chemotherapy medication irinotecan, and will find parameters for the monoclonal antibodies cetuximab and panitumumab.

A new state variable  $A$ , representing monoclonal-antibody concentration, has been created, and terms have been added to the model to include the actions of monoclonal antibodies on other types of cells in the body. We define our state variables as follows:

- Cell Populations

$T(t)$  the total tumor cell population;

$N(t)$  the concentration of NK cells per liter of blood (cells/L);

$L(t)$  the concentration of CD8<sup>+</sup>T cells per liter of blood (cells/L);

$C(t)$  the concentration of lymphocytes per liter of blood, not including NK cells and active CD8<sup>+</sup>T cells (cells/L).

- Concentrations

$M(t)$  the concentration of chemotherapy per liter of blood (mg/L);

$I(t)$  the concentration of interleukin per liter of blood (IU/liter);

$A(t)$  the concentration of monoclonal antibodies per liter of blood (mg/liter);

- Treatments:

$v_L(t)$  the number of tumor-activated CD8<sup>+</sup>T cells injected per day per liter of blood (cells/liter per day);

$v_M(t)$  the amount of irinotecan injected per day per liter of blood (mg/liter per day);

$v_A(t)$  the amount of monoclonal antibodies injected per day per liter of blood (mg/liter per day).

## 4.1 System of Equations

New terms and a new equation have been added to the ODE system given in the model by de Pillis and colleagues (2009). A summary of the purpose for each term can be found in Appendix B.1. The new ODEs of the model are given below, with changes shown in bold:

$$\begin{aligned} \frac{dT}{dt} = & aT(1 - bT) - (c + \boldsymbol{\xi} \frac{\mathbf{A}}{\mathbf{h}_1 + \mathbf{A}})NT - DT \\ & - (K_T + \mathbf{K}_{AT}\mathbf{A})(1 - e^{-\delta_T M})T - \boldsymbol{\psi}\mathbf{A}\mathbf{T} \end{aligned} \quad (4.1)$$

$$\begin{aligned} \frac{dN}{dt} = & f(\frac{e}{f}C - N) - (p + \mathbf{p}_A \frac{\mathbf{A}}{\mathbf{h}_1 + \mathbf{A}})NT + \frac{p_N NI}{g_N + I} \\ & - K_N(1 - e^{-\delta_N M})N \end{aligned} \quad (4.2)$$

$$\begin{aligned} \frac{dL}{dt} = & \frac{\theta mL}{\theta + I} + j \frac{T}{k + T}L - qLT + (r_1 N + r_2 C)T - \frac{uL^2 CI}{\kappa + I} \\ & - K_L(1 - e^{-\delta_L M})L + \frac{p_I LI}{g_I + I} + v_L(t) \end{aligned} \quad (4.3)$$

$$\frac{dC}{dt} = \beta(\frac{\alpha}{\beta} - C) - K_C(1 - e^{-\delta_C M})C \quad (4.4)$$

$$\frac{dM}{dt} = -\gamma M + v_M(t) \quad (4.5)$$

$$\frac{dI}{dt} = -\mu_I I + \phi C + \frac{\omega LI}{\zeta + I} \quad (4.6)$$

$$\frac{d\mathbf{A}}{dt} = -\boldsymbol{\eta}\mathbf{A} - \boldsymbol{\lambda}\mathbf{T} \frac{\mathbf{A}}{\mathbf{h}_2 + \mathbf{A}} + \mathbf{v}_A(\mathbf{t}) \quad (4.7)$$

where

$$D = d \frac{(L/T)^l}{s + (L/T)^l}. \quad (4.8)$$

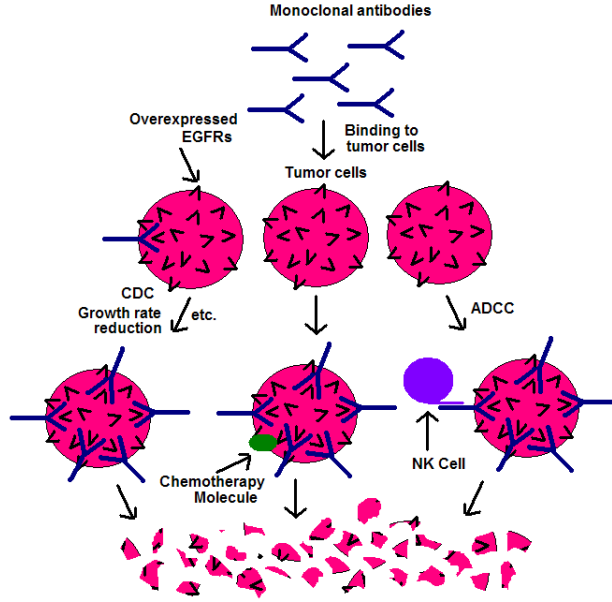


Figure 4.1: Possible pathways for MAB-induced tumor death.

## 4.2 Justifications of New Terms

The justification of all unchanged terms can be found in the 2009 paper by de Pillis and colleagues.

In Equation 4.1, three new terms have been added to represent the three pathways of MAB-induced tumor-cell death (see Figure 4.1). The term  $-\zeta \frac{A}{h_1+A} NT$  represents the rate of tumor-cell death caused by ADCC (see Section 2.2.2). Some monoclonal antibodies have protein structures which, when bound to a tumor cell, allow them to simultaneously activate NK cells and direct them to the invader (De Vita, Jr et al., 2000). Thus, when a MAB/tumor-cell complex and NK cell meet, the tumor cell is more likely to be killed than when an NK cell meets an unbound tumor cell. Kurai and colleagues (2007) found that cetuximab has a threshold concentration above which ADCC activity no longer increases. So, we assume that ADCC activity will increase with MAB concentration until it becomes saturated, and we model this with a sigmoid function. The term  $-K_{AT}A(1 - e^{-\delta_T M})T$  represents the rate of chemotherapy-induced death of tumor cells, assisted by monoclonal antibodies. When tumor cells are not able to proliferate, they are much more susceptible to chemotherapy-

induced death (De Vita, Jr et al., 2000). So, when MABs are bound to tumor cells, blocking their EGFRs and thus inhibiting tumor cell proliferation, they will increase the tumor-cell death caused by chemotherapy. The term  $-\psi AT$  will account for the rate of tumor-cell death caused by tumor cell interactions with only MABs. This term will include tumor-cell death from CDC (see Sections 2.2.1 and 2.3.2), from a reduction in EGF binding, and thus tumor-growth rate (De Vita, Jr et al., 2000), and from any other pathway currently unknown.

In Equation 4.2, one new term has been added. The term  $-p_A \frac{A}{I_1 + A} NT$  represents the rate of NK-cell death due to ADCC interactions with tumor cells and monoclonal antibodies. We assume that ADCC activity increases with MAB concentration until it becomes saturated. As with the term  $-pNT$ , it is assumed that NK cells will experience exhaustion of tumor-killing resources after interactions with tumor cells (Bhat and Watzl, 2007).

No changes were made in Equations 4.3, 4.4, and 4.5. It is worth noting, however, that we considered an additional term representing MAB-induced lymphocyte (including NK-cell and CD8<sup>+</sup>T-cell) death. Many cells, including some cells in the immune system, express EGFR. While it seems likely that the MABs would also bind to EGFRs on non tumor cells, the literature suggests that the effect of MABs is specific to tumor cells (Rodriguez et al., 2009; Martinelli et al., 2009; Gravalos et al., 2009; Siena et al., 2009; De Vita, Jr et al., 2000). Also, the usual symptoms associated with the death of quickly proliferating host cells, including hair loss and damage to the gastrointestinal tract, have not been reported as side effects of MAB treatments (De Vita, Jr et al., 2000; Martinelli et al., 2009; Gravalos et al., 2009). Tumors in colorectal cancer often overexpress only one of four growth-factor receptors, HER-1, which is the growth factor that MABs target (Gravalos et al., 2009). It is possible that the MABs affect other EGFR-presenting cells, but that blocking EGFRs on normal cells does not have a large enough effect to be detectable. Also, the majority of a MAB's pathways result in either activation of the immune system (such as ADCC or CDC) or a decrease in growth rate, and do not result directly in cell death. This may contribute to the specificity of MAB effects to tumor cells.

The only change made to Equation 4.6 was the deletion of the term  $v_I(t)$ , representing exogenous IL-2 treatment (de Pillis et al., 2009). The injection of additional cytokines has been shown to not be an effective treatment for colorectal cancer, and so does not need to be included. However the remainder of the terms were left, as endogenous interleukin is produced naturally in the body and is important in activating NK cells and CD8<sup>+</sup>T cells against (Eckert et al., 1997).

Finally, Equation 4.7 has been added to handle the model's new treatment option, injections of monoclonal antibodies. The term  $v_A(t)$  represents MAB treatments. Because MABs are not produced naturally in the body, no additional growth terms are needed. The term  $-\eta A$  represents the natural degradation of the MAB protein in the body. The term  $-\lambda T \frac{A}{h_2 + A}$  represents the loss of available MABs as they bind to tumor cells. During the chemotherapy-induced and NK-cell-induced deaths of tumor cells in MAB/tumor-cell complexes, MAB/tumor-cell binding is the first step in the process (De Vita, Jr et al., 2000), so all MABs bound to tumor cells can be included in this term, whether they are participating in ADCC, CDC, growth rate reduction, chemotherapy-induced death, or another mechanism. Because MABs have a very strong binding affinity for their target growth-factor receptors, and because there are many growth factor receptors on every cell, we assume that many MABs will be lost with each tumor cell. Also, we assume that the growth factor receptors will be fully saturated when the MAB concentration is significantly higher than the growth factor receptors. That is, we can approximate the number of MABs lost with each tumor cell as the number of growth-factor receptors on that cell, as long as MAB concentration is above a critical value to be determined in Section 5.8. To incorporate this threshold concentration, we added a saturation term similar to the one found in Equation 4.1.



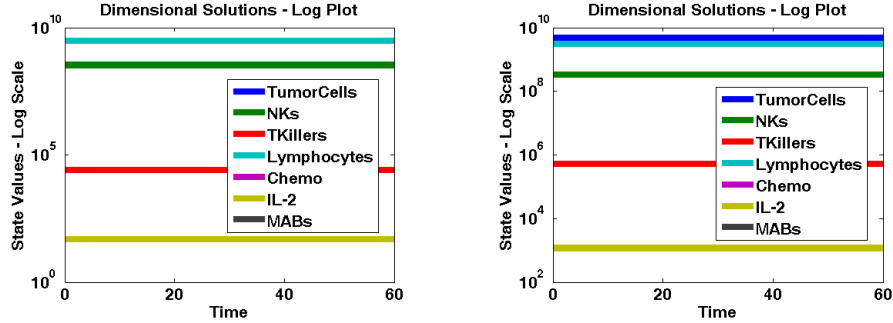
# Chapter 5

## Parameters

In order to determine parameter values, we searched peer-reviewed literature for *in vitro* and *in vivo* studies of colorectal tumor growth that could provide data for the following cases: no treatment, with irinotecan chemotherapy treatment, with cetuximab MAB treatment, and with panitumumab MAB treatment. Some of the parameters used here are those found by de Pillis and colleagues (2009) and their derivation will not be repeated here. The description of each parameter can be found in Appendix B.2 and a summary of the values used for each parameter can be found in Appendix B.3.

### 5.1 Initial Conditions

Initial conditions are determined for both a healthy individual and for the patients we will be considering, who have previously undergone treatment for their tumors. The initial values of  $N$ ,  $L$ ,  $C$ , and  $I$  can be determined for each of these patients by considering biological arguments for reasonable cell concentrations of patients with a strong and weak immune system. We assume that the healthy individual is in *homeostasis*, meaning that the cell populations will remain constant. This allows us to use the initial conditions of the healthy patient to determine where the stable equilibria in our system should be. We will then be able to plot these initial values with our system of equations to ensure that we have the desired stable equilibrium states, reflecting the realistic biological values.



(a) The *no tumor equilibrium*, for a patient with a health immune system, not receiving any treatment.

(b) The *large tumor equilibrium*, for a patient with a health immune system, not receiving any treatment.

Figure 5.1: Stable equilibria of the system.

### 5.1.1 No Tumor Equilibrium with a Strong Immune System

We first calculated initial conditions for a healthy patient with no tumor ( $T = 0$ ) and receiving no cancer treatments ( $M = A = 0$ ) to find a *no tumor equilibrium*. Because we are assuming that the healthy patients are in homeostasis, we can set each time derivative equal to zero. We found  $N$  and  $C$  by assuming a lymphocyte count of  $3.333 \times 10^9$  cells, which is within the range for a normal lymphocyte count, and assuming natural killer and  $CD8^+$  T cell counts to be 10 percent and  $< 1$  percent, respectively (Abbas and Lichtman, 2005). This gives us that  $C = 3.333 \times 10^9 \times 0.9 = 3 \times 10^9$  and  $N = 3.333 \times 10^9 \times 0.1 = 3.333 \times 10^8$ . The values for  $L$  and  $I$  are taken from de Pillis's team (2009), who derives  $L$  from Pittet's team 1999 and Speiser's team (2001), and  $I$  from Orditura's team (2000) and information provided by Novartis Pharmaceuticals (2007). These calculations give us the following values for our *no tumor equilibrium*:

$$T = 0, N = 3.333 \times 10^8, L = 2.526 \times 10^4, C = 3 \times 10^9, M = 0,$$

$$I = 48.9273, A = 0.$$

After parameter values were found, we were able to show graphically that these initial conditions appear to correspond to a stable equilibrium state of the system (see Figure 5.1(a)).

### 5.1.2 Large Tumor Equilibrium with a Strong Immune System

We next calculated initial conditions for a healthy individual who has a large tumor but is not receiving any treatment ( $M = A = 0$ ). We again set the time derivatives to zero under the assumption of homeostasis. Under conditions of an untreated tumor, we leave  $N$  and  $C$  at the same values, but use larger values for  $I$  and  $L$ , since the presence of a tumor increases the production of cytokines. We take the values of  $I = 1173$  and  $L = 5.268 \times 10^5$  from de Pillis and colleagues (2009), who derive  $L$  from Lee's team (1999) and Janeway's book on *Immunobiology* (2005), and  $I$  again from Orditura's team (2000) and information provided by Novartis Pharmaceuticals (2007). With these initial values and the parameters that can be directly calculated from available literature, we solve for the size of a large tumor in equilibrium while solving for the parameter  $p$  in Section 5.3. Note that the resulting value,  $T = 4.65928 \times 10^9$ , is slightly less than the theoretical carrying capacity of  $4.66 \times 10^9$  which we find during the calculation of the parameter  $b$  in Section 5.2. This is expected, because interactions with the immune system prevent the tumor from reaching its theoretical carrying capacity. These initial values give us the following *large tumor equilibrium*:

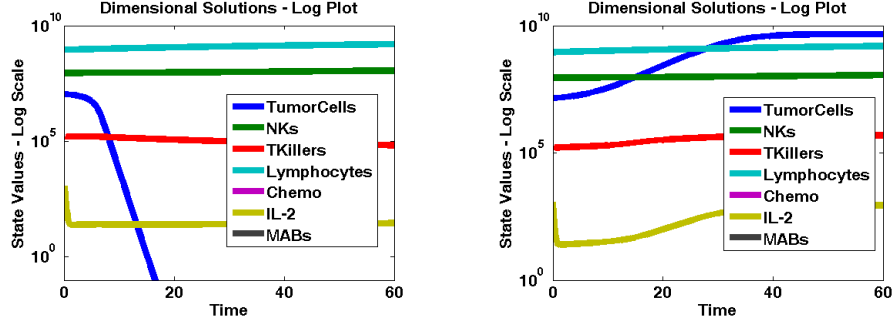
$$T = 4.65928 \times 10^9, N = 3.333 \times 10^8, L = 5.268 \times 10^5, C = 3 \times 10^9,$$

$$M = 0, I = 1173, A = 0.$$

We were again able to show graphically that these initial conditions appear to correspond to a stable equilibrium state of the system (see Figure 5.1(b)).

### 5.1.3 Initial Conditions for a Weakened Immune System

Because the majority of the patients we were considering had previously undergone various treatments and did not have very strong immune systems, we reduced the initial values for  $N$ ,  $L$ , and  $C$  in our simulations. We used an initial value of  $C = 10^9$  for the lymphocyte population. This value is within the normal range for lymphocyte concentration, but is very close to being low (Abbas and Lichtman, 2005). We considered  $N$  and  $L$  to be a slightly lower percentage of total lymphocytes than in a healthy individual, and set  $N = 9 \times 10^7$  and  $L = 5 \times 10^4$ . These two populations, the natural killer cells and activated CD8<sup>+</sup>T cells, interact more directly with the tumor than the other lymphocytes, so we assume that they are deactivated at a slightly higher rate. Initial values for  $M$  and  $A$  are set to zero, but  $\frac{dM}{dt}$  and



(a)  $T(0) = 1.1 \times 10^7$  cells. A tumor with a small initial size will quickly shrink to zero.

(b)  $T(0) = 1.4 \times 10^7$  cells. A tumor with a large initial size will quickly grow to the carrying capacity of the system.

Figure 5.2: Patients who begin at our initial conditions can end up at either the *no tumor equilibrium* or the *large tumor equilibrium*.

$\frac{dA}{dt}$  will be nonzero at any time  $t$  when the patient is receiving treatments. Because the presence of tumors fragments stimulate IL-2 production (Sompayrac, 2008), we leave  $I = 1173$  as the initial value for  $I$ . The initial value of  $T$  can be varied, and will be stated with simulations. These calculations give us the following initial conditions for the other populations in our model:

$$N(0) = 9 \times 10^7, L(0) = 5 \times 10^4, C(0) = 10^9, M(0) = 0,$$

$$I(0) = 1173, A(0) = 0.$$

These initial values represent patients who are not in homeostasis, and depending on the initial tumor size, the strength of interactions between the patient's immune system and the tumor, and whether any medication is given, their cell populations can be driven either to the *no tumor equilibrium* or to the *large tumor equilibrium*. Sample conditions for a tumor that is reduced to the *no tumor equilibrium* can be seen in Figure 5.2(a), and sample conditions for a tumor that grows to the *large tumor equilibrium* can be seen in Figure 5.2(b).

## 5.2 $\frac{dT}{dt}$ : The Tumor

$a = 2.31 \times 10^{-1} \text{ day}^{-1}$ , the tumor growth rate, was calculated from the doubling time of colorectal tumors during exponential growth, which was found by Corbett's team (1975) to be 3 days. We can calculate  $a$  from the equation for exponential growth with a half-life of  $t = 3$  days. So,  $2t_0 = t_0 e^{at}$ , giving us that  $a = \frac{\ln(2)}{3} = 2.31 \times 10^{-1}$ . This is approximately half of the value for  $a$  found by de Pillis's team (2009), but colon tumors are known to have slower growth rates than most types of cancer, so this is not an unreasonable value (Bolin et al., 1983; Burnett and Greenbaum, 1981). It is important to note that Corbett's team grew their tumors in non immunodeficient mice. However this, was the only study in our literature search that provides the doubling time specifically during exponential growth. The growth rate that we calculated is comparable to the value found by de Pillis and colleagues (2009), and also agrees with the initial growth rates found by Leith's team (1987), who grew colon tumors in immunodeficient mice.

$b = 2.146 \times 10^{-10} \text{ cells}^{-1}$ , is the inverse of the carrying capacity. The carrying capacity (in volume) of colorectal tumors was taken from Leith and colleagues (1987), who collected tumor growth data, fit them to the Gompertz equation, and found the maximum tumor size as  $t \rightarrow \infty$ . The carrying capacity derived from the Gompertz model has the same biological interpretation as in our model, so we were able to use the results of Leith's team to find a value for  $b$ . Multiple carrying capacities were found from different colorectal tumor lines, with an average of approximately  $10,000 \text{ mm}^3 = 10^{13} \mu\text{m}^3$ . This size was then converted to a cell population using  $2145 \mu\text{m}^3$  as the average tumor cell volume (Chen et al., 2005), giving  $10^{13} \mu\text{m}^3 / (2145 \mu\text{m}^3 / \text{cell}) = 4.66 \times 10^9$  cells. Thus,  $b = (4.66 \times 10^9 \text{ cells})^{-1} = 2.146 \times 10^{-10}$ .

$c = 5.156 \times 10^{-14} \text{ L cells}^{-1} \text{ day}^{-1}$ , the rate of NK-induced tumor death, is set equal to  $p$  (see Section 5.3) as was done by de Pillis's team de Pillis et al. (2009). Recent research (Bhat and Watzl, 2007) suggests that natural killer cells may be able to kill up to six tumors before deactivation. However we have not found further confirmation of this and so have chosen to continue using the assumption that NK cells are only able to kill one tumor cell each.

$D = d \frac{(L/T)^l}{s+(L/T)^l}$  involves three parameters, to which we assign four separate values each, in order to reflect a variety of patient-specific states. These parameters are:  $d$  ( $\text{day}^{-1}$ ), the immune-system strength coefficient;  $l$ , the immune-system strength scaling coefficient; and  $s$  (L), the value of  $(\frac{L}{T})^l$  necessary for half-maximal  $\text{CD8}^+$  T-cell toxicity. We base our values for  $d$ ,  $l$ , and  $s$  on the values used by de Pillis and colleagues (2009), however we slightly lower  $d$  and  $l$  and slightly raise  $s$  to represent that many of our patients are not in very good health and have gone through multiple cancer treatments. We use  $d \in \{1.3, 1.6, 1.9, 2.1\}$ ,  $l \in \{1.1, 1.4, 1.7, 2.0\}$ , and  $s \in \{4 \times 10^{-3}, 7 \times 10^{-3}, 9 \times 10^{-3}, 3 \times 10^{-2}\}$ , which results in sixty-four different “patients” over which we can run simulations to represent clinical trials.

$\zeta = 6.5 \times 10^{-10} \text{ L cells}^{-1} \text{ day}^{-1}$  for cetuximab, and  $= 0$  for panitumumab, is the rate of NK-induced tumor death through ADCC. The value for cetuximab was set to match the expected increase in NK cell activity found by Kurai and colleagues (2007). Kurai’s team varied concentrations of tumor cells and NK cells, left them for 4 hours with and without  $0.25 \mu\text{g}/\text{mL}$  cetuximab, and measured the resulting NK activity. They measured the activity at much higher concentrations of NK cells than are present in the body, but based on their results we approximated that at the ratio of one NK cell: ten tumor cells, NK activity is increased by 10 percent. We found an appropriate value for  $\zeta$  by running simulations up to  $t = 4$  hours,  $T_0 = 10^9$ ,  $N_0 = 2.5 \times 10^8$ , and an initial treatment of  $0.25 \text{ mg}/\text{L}$  cetuximab over 15 minutes. The other immune system components, as well as natural growth and decay, were ignored. A value of  $\zeta = 6.5 \times 10^{-10}$  was found to give the desired 10 percent decrease in NK cells, which we use as a proxy for an increase in NK activity of 10 percent. Panitumumab is unable to activate the ADCC pathway, so  $\zeta$  is set to zero in that case (Grothey, 2006).

$h_1 = 1.25 \times 10^{-6} \text{ mg L}^{-1}$  for cetuximab, and  $0$  for panitumumab, is the concentration of MABs necessary for a half-maximal increase in ADCC. The ADCC activity level indicated by  $\zeta$  is reached when the cetuximab concentration is above  $0.25 \mu\text{g}/\text{mL}$ , and so  $h_1$  was set to  $.5 \times 0.25 \mu\text{g}/\text{mL} = 1.25 \times 10^{-6} \text{ mg}/\text{L}$ . Cetuximab levels in the body are usually above this threshold during treatment (at about one fiftieth of a normal dose), and we chose to use a sigmoid function to capture this threshold. Although we do not have evidence supporting

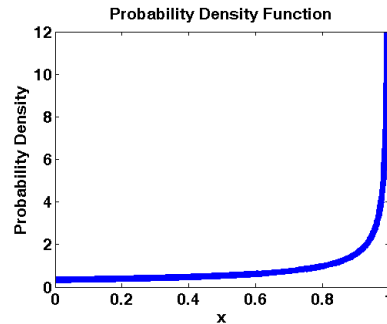


Figure 5.3: The probability density function of  $x$  and  $y$ .

that ADCC activity increases according to a saturation function, this model captures the two important characteristics: that the threshold concentration for maximal ADCC activity is much lower than the normal cetuximab dose, and that the ADCC activity level approaches zero as MAB concentration approaches zero. We chose  $h_1$  so that, when the cetuximab concentration is half of the threshold value, the term  $\frac{A}{h_1+A}$  will be one half, resulting in half-maximal ADCC activity. Because panitumumab does not play a role in ADCC, panitumumab does not have an  $h_1$ .

$K_T = (8.1 \times 10^{-1})x \text{ day}^{-1}$  is the rate of chemotherapy-induced tumor death, where  $x$  is a random variable with the *probability density function* (the likelihood of  $x$  taking on each value) shown in Figure 5.3. We chose this random variable because we wanted  $x \in [0, 1]$ . Also, we wanted  $x$  to be close to one most of the time, and this random variable has an *expected value* (mean value) of  $E[x] = 0.75$ . Therefore,  $K_T \in [0, 8.1 \times 10^{-1}]$ , and has a mean value of  $K_T = 6.075 \times 10^{-1}$ . Multiplying the maximum value for  $K_T$  by this random variable allows us to represent that each tumor is affected differently by chemotherapy medications. Each patient (each simulation) will have one constant value for  $K_T$ , but a different  $K_T$  will be randomly generated for every patient.

The maximal value of  $K_T$  was calculated from *in vitro* data collected by Vilar and colleagues (2006) on irinotecan concentration and growth reduction of various colon cancer cell strains. We chose to use values from the HT-29 cell line, as many of our other references used this cell line also. We estimated five coordinates from a plot presented by

Vilar's team which gave irinotecan concentration (in mol/L) versus growth of tumor cells, as a percentage of tumor cell growth with no irinotecan. Since this was an *in vitro* study run over the course of only a few days, we set all but tumor size and chemotherapy concentration to zero and considered natural cell death to be zero. We also assumed that chemotherapy concentration would be held constant, so  $\frac{dM}{dt} = 0$ . Thus our equation for tumor size becomes  $\frac{dT}{dt} = -K_T(1 - e^{-\delta_T M})T$ , and so  $T = T_0 e^{-K_T(1 - e^{-\delta_T M})t}$ . We converted the irinotecan concentration at each point to units of mg/L using 677 g/mol as the molecular weight of irinotecan (Tsuruo et al., 1988). We then used tumor sizes and chemotherapy concentrations from each point to write five equations with  $\delta_T$  and  $K_T$  as unknowns. Since the system is overdetermined (five equations, two unknowns), we chose values for  $\delta_T$  and  $K_T$  that produced a reasonable fit. We found  $\delta_T = 0.2$  and  $K_T \approx 0.85$ .

$K_T$  was then separately confirmed by running multiple simulations with our set of patient-specific parameter values to look for a tumor response rate of approximately 10 percent after 6 weeks of treatment. The reported *response rate*, the percentage of patients whose tumor did not continue to grow after treatment, for irinotecan is around 30 percent, however patients receiving MAB treatment have usually already received a variety of chemotherapy treatments and did not respond strongly to them (De Vita, Jr et al., 2000). Additionally, a 10 percent difference is reported between response rates for MAB therapy alone and MAB/chemotherapy combinations, so we made this percentage our goal instead of 30 percent (De Vita, Jr et al., 2000). These simulations confirmed that a value of  $K_T = 0.81$  gives an average response rate of approximately 10 percent.

$K_{AT} = 4 \times 10^{-4} \text{ L mg}^{-1} \text{ day}^{-1}$  for both cetuximab and panitumumab, is the additional chemotherapy-induced tumor death due to MAB-tumor interactions. Even with  $K_{AT}$  set to zero, combination treatments give us a response rate approximately 85 percent after 4 weeks of cetuximab and irinotecan treatments, and approximately 75 percent after 6 weeks of panitumumab and irinotecan treatments, compared to the expected response rates of 22.5 percent for cetuximab/irinotecan therapy and 20 percent for panitumumab/irinotecan therapy (De Vita, Jr et al., 2000; Gravalos et al., 2009). However, it is known that MAB therapy can help to increase chemotherapy responses in tumors, and even restore partial response in chemotherapy-refractory tumors, and

we chose a value of  $K_{AT} = 4 \times 10^{-4}$  (De Vita, Jr et al., 2000). At maximal MAB concentrations, which are on the order of  $10^2$ , this will result in an increase in chemotherapy activity of approximately  $\frac{4 \times 10^{-4} \times 10^2}{8.1 \times 10^{-1}} \approx .05 = 5\%$ . If the simulations are run for 100 days with  $K_{AT} = 4 \times 10^{-4}$ , we get an overall result of approximately 10 percent of tumors reduced or eradicated, which seems reasonable.

$\delta_T = 2 \times 10^{-1} \text{ L mg}^{-1}$ , the medicine efficacy coefficient, was found as part of the calculation for  $K_T$ .

$\psi = (2.28 \times 10^{-2})y \text{ L mg}^{-1}\text{day}^{-1}$  for cetuximab and  $= (2.58 \times 10^{-2})y \text{ L mg}^{-1}\text{day}^{-1}$  for panitumumab is the rate of MAB-induced tumor death, where  $y$  is a random variable with the same properties as  $x$ , chosen for the same reasons (see description of  $K_T$  and Figure 5.3). Therefore, for cetuximab  $\psi \in [0, 2.28 \times 10^{-2}]$ , with a mean value of  $1.71 \times 10^{-2}$ , and for panitumumab  $\psi \in [0, 2.58 \times 10^{-2}]$ , with a mean value of  $1.94 \times 10^{-2}$ . As with  $K_T$ , multiplying the maximum value for  $\psi$  by a random variable between zero and one allows us to represent that each tumor has a different response to treatments. Each patient (each simulation) will have one constant value for  $\psi$ , but a different  $\psi$  will be randomly generated for every patient.

After other parameters for MAB monotherapy had been calculated, the maximal value of  $\psi$  for each medication was found by running simulations of MAB therapy as a single treatment over our set of patient-specific parameters with a range of values for  $\psi$ , until we achieved the desired response rate. We found  $\psi$  such that the response rate for cetuximab after four weeks of treatment is 10 percent and the response rate for panitumumab after six weeks of treatment is 13 percent (De Vita, Jr et al., 2000).

### 5.3 $\frac{dN}{dt}$ : Natural Killer Cells

$\frac{e}{f} = \frac{1}{9}$ , the ratio of the NK cell synthesis rate to the turnover rate, is found using the same method as de Pillis's team (2009). The value for  $\frac{e}{f}$  is found by assuming the *no tumor equilibrium* and thus setting Equation 4.2 to zero. We then ignore the term  $\frac{p_N N I}{g_N + I}$ , which has only a very small effect on NK proliferation. It is approximately equal to the ratio of NK cells/other lymphocytes, where other lymphocytes corresponds to our C state and does not include activated T cells or NK

cells. As in Section 5.1, NK cells make up approximately 10 percent of all lymphocytes, and T cell count is negligible, giving us  $\frac{10\%}{90\%}$ , or  $\frac{1}{9}$  (Abbas and Lichtman, 2005).

$f = 1 \times 10^{-2} \text{ day}^{-1}$ , the rate of NK cell turnover, is based on the value of  $f = 1.25 \times 10^{-2}$  found by de Pillis and colleagues (2009). We lowered the value slightly to agree with our assumption of a patient with a weakened immune system, whose body may not be able to produce new cells as quickly as normal healthy individual.

$g_N = 2.5036 \times 10^5 \text{ IU L}^{-1}$ , the concentration of IL-2 needed for half-maximal NK cell proliferation, is unchanged from the value found by de Pillis's team (2009).

$p_N = 5.13 \times 10^{-2} \text{ day}^{-1}$ , the rate of IL-2 induced NK cell proliferation, is calculated using the same method as de Pillis's team (2009). They use data from Meropol and colleagues (1998) to find that  $5.0073 \times 10^4 \text{ IU}$  stimulates NK cells to reach a count of  $2.3 \times 10^9$  cells, and so using these as  $I$  and  $N$  respectively and assuming  $T = 0$ , we then set Equation 4.2 equal to zero and solve for  $p_N$ :

$$p_N = \frac{f(N - \frac{e}{f}C)(g_N + I)}{NI}.$$

Using  $C = 3 \times 10^9$  from our *no tumor equilibrium* (see Section 5.1.1) and the previously calculated values for  $e$ ,  $f$ , and  $g_N$ , we find that  $p_N = 5.13 \times 10^{-2}$ .

$p = 5.156 \times 10^{-14} \text{ L cells}^{-1} \text{ day}^{-1}$ , the rate of NK cell death due to tumor interaction, is calculated using the same method as de Pillis's team (2009). We consider the *large tumor equilibrium* with no medication, which allows us to set Equations 4.1 and 4.2 equal to zero and to solve for  $T$  and  $p$ :

$$\begin{aligned} p &= \frac{\frac{p_N NI}{g_N + I} + eC - fN}{NT} \text{ and} \\ 0 &= aT(1 - bT) - cNT - DT \\ &= aT(1 - bT) - pNT - DT. \end{aligned}$$

We were then able to use the values for  $p_N$ ,  $g_N$ ,  $e$ ,  $f$ ,  $a$ ,  $b$ , the equation for  $D$  with the parameters described in Section 6, and the state values

for the immune system populations from the *large tumor equilibrium* to find that  $T = 4.65928 \times 10^9$  in the *large tumor equilibrium* and  $p = 5.156 \times 10^{-14}$ .

$p_A = 6.5 \times 10^{-10}$  L cells<sup>-1</sup>day<sup>-1</sup> for cetuximab and 0 for panitumumab is the rate of NK cell death due to interactions with MAB-tumor complexes. We set  $p_A = \zeta$ , under the approximation used for the parameter  $c$  in Section 5.2 that for each tumor cell killed through ADCC, one NK cell will also die.

$K_N = 9.048 \times 10^{-1}$  day<sup>-1</sup>, the rate of NK depletion from chemotherapy toxicity, is calculated using the same method as de Pillis's team (2009), by linearly scaling  $K_C$  by the ratio of cell metabolic rates (see Section 5.5 for  $K_C$  calculation). That is,

$$K_N = \frac{f}{\beta} K_C.$$

$\delta_N = 2 \times 10^{-1}$  L mg<sup>-1</sup>, the chemotherapy toxicity coefficient, is assumed to equal  $\delta_T$ . The drug has a different efficacy ( $K$ ) for each cell type, but we assume that a similar concentration of irinotecan is needed to affect each cell, regardless of cell type (de Pillis et al., 2009).

#### 5.4 $\frac{dL}{dt}$ : CD8<sup>+</sup>T cells

$m = 5 \times 10^{-3}$  day<sup>-1</sup>, the rate of activated CD8<sup>+</sup>T-cell turnover, is based on the value of  $m = 9 \times 10^{-3}$  found by de Pillis and colleagues (2009). We lowered the value slightly to agree with our assumption of a patient with a weakened immune system, whose body may not be able to produce new cells as quickly as normal healthy individual.

$\theta = 2.5036 \times 10^{-3}$  IU L<sup>-1</sup>, the concentration of IL-2 to half CD8<sup>+</sup>T-cell turnover, is unchanged from de Pillis and colleagues (2009).

$q = 5.156 \times 10^{-17}$  cells<sup>-1</sup>day<sup>-1</sup>, the rate of CD8<sup>+</sup>T-cell death due to tumor interaction, is set equal to  $p \times 10^{-3}$  because, as de Pillis and colleagues (2009) point out, we expect  $q$  to be approximately three orders of magnitude less than  $p$  since  $L$  is approximately three orders of magnitude less than  $N$ .

$r_1 = 5.156 \times 10^{-12} \text{ cells}^{-1}\text{day}^{-1}$ , the rate of NK-lysed tumor cell debris activation of CD8<sup>+</sup>T cells, is calculated using the same method as de Pillis's team (2009). We set  $r_1 = 100 \times c$ , based on the approximated a lysed tumor cell can stimulated 10-300 T cells per day (de Pillis et al., 2009).

$r_2 = 1 \times 10^{-15} \text{ cells}^{-1}\text{day}^{-1}$ , the rate of CD8<sup>+</sup>T-cell production from circulating lymphocytes, is based on the value of  $r_2 = 5.8467 \times 10^{-13}$  found by de Pillis and colleagues (2009). We reduced it from their value to reflect that a weak immune system may not be able to produce activated CD8 cells as effectively.

$p_I = 2.4036 \text{ day}^{-1}$ , the rate of IL-2 induced CD8<sup>+</sup>T-cell activation, was found using the same method as de Pillis's team (2009). A system of equations was created by considering the no tumor equilibrium and the large tumor equilibrium (see Sections 5.1.1 and 5.1.2). Setting Equation 4.3 to zero and using to two sets of initial values for  $T$ ,  $N$ ,  $L$ ,  $C$ , and  $I$ , we can obtain two equations each with  $p_I$  and  $u$  as unknowns, and thus solve for the  $p_I$  and  $u$  necessary to make satisfy the equilibrium conditions.

$g_I = 2.5036 \times 10^3 \text{ IU L}^{-1}$ , the concentration of IL-2 necessary for half-maximal CD8<sup>+</sup>T-cell activation, is unchanged from the value found by de Pillis's team (2009).

$u = 3.1718 \times 10^{-14} \text{ L}^2 \text{ cells}^{-2}\text{day}^{-1}$ , the CD8<sup>+</sup>T-cell self-limitation feedback coefficient, is obtained from the system of equations used to calculate  $p_I$ .

$\kappa = 2.5036 \times 10^3 \text{ IU L}^{-1}$ , the concentration of IL-2 to halve the magnitude of CD8<sup>+</sup>T-cell self-regulation, is unchanged from the value found by de Pillis's team (2009).

$j = 1.245 \times 10^{-4} \text{ day}^{-1}$ , the rate of CD8<sup>+</sup>T-cell lysed tumor cell debris activation of CD8<sup>+</sup>T cells, is based on the value of  $1.245 \times 10^{-2}$  found by de Pillis and colleagues (2009), and was decreased to indicate that the weak immune system may not be able to activate CD8 cells as effectively.

$k = 2.019 \times 10^7 \text{ cells}$ , the tumor size for half-maximal CD8<sup>+</sup>T-cell lysed tumor debris CD8<sup>+</sup>T cell activation, is unchanged from the value found by de Pillis's team (2009).

$K_L = 4.524 \times 10^{-1} \text{ day}^{-1}$ , the rate of CD8<sup>+</sup>T-cell depletion from chemotherapy toxicity, is found in the same way as we found  $K_N$ . We calculated it using the same method as de Pillis's team (2009), by linearly scaling  $K_C$ . That is,

$$K_L = \frac{m}{\beta} K_C.$$

$\delta_L = 2 \times 10^{-1} \text{ L mg}^{-1}$ , the chemotherapy toxicity coefficient, is found in the same way as we found  $\delta_N$ . We assumed it to be equal to  $\delta_T$  (de Pillis et al., 2009).

## 5.5 $\frac{dC}{dt}$ : Lymphocytes

$\frac{\alpha}{\beta} = 3 \times 10^9 \text{ cells L}^{-1}$ , the ratio of the rate of circulating lymphocyte production to turnover rate, is taken from considering the steady state assumption of  $\frac{dC}{dt} = 0$  in a healthy, tumor free individual. Considering Equation 4.4 with  $M = 0$ , we find that  $\frac{\alpha}{\beta} = C$ , where  $C = 3 \times 10^9$  refers to the equilibrium value of  $C$  in the *no tumor equilibrium* (see Section 5.1).

$\beta = 6.3 \times 10^{-3} \text{ day}^{-1}$ , the rate of lymphocyte turnover, is unchanged from the value found by de Pillis's team (2009).

$K_C = 5.7 \times 10^{-1} \text{ day}^{-1}$ , the rate of lymphocyte depletion from chemotherapy toxicity, was calculated to achieve the results given by Catimel and colleagues (1995) on the number of patients with leukopenia after irinotecan treatments. Catimel's team found that when  $100 \text{ mg/m}^2$  was given to patients daily for three days, three out of eleven patients had leukopenia, and when  $115 \text{ mg/m}^2$  was given daily for three days, four out of ten patients had leukopenia. We assumed that the normal leukocyte count is  $4.5 - 11 \times 10^9 \text{ cells/L}$ , and lymphocytes can make up 16-46 percent of the total leukocytes in the body (Abbas and Lichtman, 2005). Thus, we calculate that the normal lymphocyte count is  $0.72 - 5.06 \times 10^9 \text{ cells/L}$ . A patient is considered to have leukopenia when the leukocyte count drops below  $1.9 \times 10^9$  (Welink et al., 1999), and so the highest possible lymphocyte count in a patient with leukopenia is 46 percent of  $1.9 \times 10^9$ , or  $8.74 \times 10^8$  cells. We will assume that the lymphocyte count for all patients will drop equally, and so those who begin initially with a lower lymphocyte count will become leukopenic, and those who begin with a higher lymphocyte

count will have a reduced cell count, but will remain within the normal range. So, the lowest three elevenths of patients will have lymphocyte levels below  $1.904 \times 10^9$  cells, and the lowest four tenths of patients will have lymphocyte levels below  $2.456 \times 10^9$  cells. We ran simulations considering only lymphocyte counts, with irinotecan delivered once daily over 1.5 hours for a total of 3 days, and found a value for  $K_C$  that made an initial lymphocyte count of  $1.904 \times 10^9$  drop to approximately  $8.74 \times 10^8$  with a  $100 \text{ mg/m}^2$  dose and an initial lymphocyte count of  $2.456 \times 10^9$  drop to approximately  $8.74 \times 10^8$  with a  $115 \text{ mg/m}^2$  dose. The two doses resulted in  $K_C$  values of 0.52 and 0.63 respectively, so these were averaged to find  $K_C = .57$ .

$\delta_C = 2 \times 10^{-1} \text{ L mg}^{-1}$ , the chemotherapy toxicity coefficient, is found in the same way as we found  $\delta_L$ . We assumed it to be equal to  $\delta_T$  (de Pillis et al., 2009).

## 5.6 $\frac{dM}{dt}$ : Irinotecan Chemotherapy Treatment

$\gamma = 4.077 \times 10^{-1} \text{ day}^{-1}$ , the rate of excretion and elimination of chemotherapy drug, is calculated using the assumption of exponential decay from  $\frac{\ln(2)}{t_{1/2}}$ , where  $t_{1/2}$  is the half-life of SN-38, the active form of irinotecan, in tissue. We found that the half-life of irinotecan in rat tissue is 7.2 hours, the half life of irinotecan in rat plasma is 1.8 hours, the half life of irinotecan in human plasma is 8.3 hours, and the half life of SN-38 in human plasma is 10.2 hours (Noble et al., 2006; Catimel et al., 1995). We then assume that the ratio of the irinotecan half life in rat tissue/rat plasma equals the ratio of irinotecan half life in human tissue/human plasma, to get that the half life of irinotecan in human tissue is  $7.2 \times 8.3/1.8 = 33.2$  hours. We also assume that the ratio of irinotecan half life in human tissue/plasma equals the SN-38 half life in human tissue/plasma, which gives us that the half life of SN-38 in human tissue is  $33.2 \times 10.2/8.3 = 40.8$  hours. Thus  $\gamma = \frac{\ln(2)}{40.8/24} = 4.077 \times 10^{-1}$ .

## 5.7 $\frac{dI}{dt}$ : Interleukin

$\mu_I = 11.7427 \text{ day}^{-1}$ , the rate of excretion and elimination of IL-2, is unchanged from the value found by de Pillis's team (2009).

$\omega = 7.88 \times 10^{-2}$  IU cells<sup>-1</sup>day<sup>-1</sup>, the rate of IL-2 production from CD8<sup>+</sup>T cells, is calculated using the same method as de Pillis's team (2009), from the no tumor and large tumor equilibria.  $\frac{dI}{dt}$  is set to zero, and the known parameters and initial values are used to find two equations with  $\omega$  and  $\phi$  unknown. These two parameters can then be solved for.

$\phi = 1.788 \times 10^{-7}$  IU cells<sup>-1</sup>day<sup>-1</sup>, the rate of IL-2 production from CD4<sup>+</sup> and naive CD8<sup>+</sup>T-cell IL-2 production, is found as part of the system of equations solving for  $\omega$ .

$\zeta = 2.5036 \times 10^3$  IU L<sup>-1</sup>, the concentration of IL-2 for half-maximal CD8<sup>+</sup>T-cell IL-2 production, is unchanged from the value found by de Pillis's team (2009).

## 5.8 $\frac{dA}{dt}$ : Cetuximab and Panitumumab Monoclonal Antibody Treatment

$\eta = 1.386 \times 10^{-1}$  day<sup>-1</sup> for cetuximab and  $9.242 \times 10^{-2}$  day<sup>-1</sup> for panitumumab is the rate of MAB turnover and excretion. The parameter  $\eta$  is calculated using the assumption of exponential decay from  $\frac{\ln(2)}{t_{1/2}}$ , where  $t_{1/2}$  is the half-life in tissue of each MAB. For cetuximab, the half life in tissue is 5 days, so  $\eta = \frac{\ln(2)}{5} = 0.139$  (Grothey, 2006). For panitumumab, the half life in tissue is 7.5 days, so  $\eta = \frac{\ln(2)}{7.5} = 0.092$  (Grothey, 2006).

$\lambda = 8.3 \times 10^{-14}$  mg cells<sup>-1</sup>L<sup>-1</sup>day<sup>-1</sup> for cetuximab and  $8.6 \times 10^{-14}$  mg cells<sup>-1</sup>L<sup>-1</sup> day<sup>-1</sup> for panitumumab is the rate of MAB/tumor-cell complex formation. Average cells have around 20,000 EGFRs (American Association for Cancer Research, 2010). The binding affinity of cetuximab is 400 pM (picomolar, which measures the ratio of the concentration of unbound molecules to the concentration of bound molecules) and for panitumumab it is 50 pM (Freeman et al., 2008). We will first consider cetuximab, which has a molecular weight of 152 kD=152 × 10<sup>6</sup> mg/mol (RxList, 2009a). A binding affinity of 400 pM means that 400 pM = [cetuximab][EGFRs]/[cetuximab-EGFR complexes]. To find the number of cetuximab-EGFR complexes per cell,

we first converted 400 pM to units of mg/L:

$$\frac{400 \text{ pmol}}{1\text{L}} \times \frac{1 \text{ mol}}{10^{12} \text{ pmol}} \times \frac{152 \times 10^6 \text{ mg}}{1\text{mol}} = 6.08 \times 10^{-2} \text{ mg/L.}$$

This is approximately one sixteenth, so for each free cetuximab molecule and EGFR, there are about sixteen cetuximab-EGFR complexes. So, out of 20,000 EGFRs, approximately 1250 of them will be free, and therefore 18750 cetuximab molecules will be lost for each tumor cell lost. We can convert this back into concentration of cetuximab lost per tumor cell:

$$18,750 \text{ MABs} \times \frac{1 \text{ mol}}{6 \times 10^{23} \text{ MABs}} \times \frac{152 \times 10^6 \text{ mg}}{1 \text{ mol}} \times \frac{1}{57\text{L}} \\ = 8.3 \times 10^{-14} \text{ mg/L.}$$

Thus, for cetuximab,  $\lambda = 8.3 \times 10^{-14}$ . For panitumumab, we will do a similar computation, using instead panitumumab's binding affinity and its molecular weight of 147 kD= $147 \times 10^6$  mg/mol (RxList, 2009b). We will first change units on the binding affinity to the units of panitumumab concentration:

$$\frac{50 \text{ pmol}}{1\text{L}} \times \frac{1 \text{ mol}}{10^{12} \text{ pmol}} \times \frac{147 \times 10^6 \text{ mg}}{1\text{mol}} = 7.35 \times 10^{-3} \text{ mg/L.}$$

This is approximately  $\frac{1}{136}$ , so for each free panitumumab molecule and EGFR, there are about 136 panitumumab-EGFR complexes. So, out of 20,000 EGFRs, approximately 147 of them will be free, and therefore about 19,850 panitumumab molecules will be lost for each tumor cell lost. We can convert this back into mg of panitumumab lost per tumor cell:

$$19,850 \text{ MABs} \times \frac{1 \text{ mol}}{6 \times 10^{23} \text{ MABs}} \times \frac{147 \times 10^6 \text{ mg}}{1 \text{ mol}} \times \frac{1}{57\text{L}} \\ = 8.6 \times 10^{-14} \text{ mg/L.}$$

Thus for panitumumab,  $\lambda = 8.6 \times 10^{-14}$ .

$h_2 = 4 \times 10^{-5} \text{ mg L}^{-1}$  for cetuximab and  $4.05 \times 10^{-5} \text{ mg L}^{-1}$  for panitumumab is the concentration of MABs for half-maximal EGFR binding. We will first consider cetuximab, and will use  $10^9$  as the number

of tumor cells and 57 L as the volume of an average person (de Pillis et al., 2009). Assuming that 18,750 cetuximab molecules bind to each tumor cell, we want to find the number of mg/L at which the EGFRs are saturated:

$$\frac{18,750 \text{ MAB}}{1 \text{ cell}} \times 10^9 \text{ tumor cells} \times \frac{1 \text{ mol}}{6 \times 10^{23} \text{ MAB}} \times \frac{152 \times 10^6 \text{ mg}}{1 \text{ mol}} \times \frac{1}{57 \text{ L}} = 8.0 \times 10^{-5} \text{ mg/L}.$$

So, we will set  $h_2 = 0.5 \times 8 \times 10^{-5} = 4 \times 10^{-5}$  mg/L for cetuximab. We will do a similar computation for panitumumab, using instead 19,850 MABs for each cell:

$$\frac{19850 \text{ MAB}}{1 \text{ cell}} \times 10^9 \text{ tumor cells} \times \frac{1 \text{ mol}}{6 \times 10^{23} \text{ MAB}} \times \frac{147 \times 10^6 \text{ mg}}{1 \text{ mol}} \times \frac{1}{57 \text{ L}} = 8.1 \times 10^{-5} \text{ mg/L}.$$

Thus we will set  $h_2 = 0.5 \times 8.1 \times 10^{-5} = 4.05 \times 10^{-5}$  mg/L for panitumumab.

## 5.9 Treatments

In this section we show the calculations performed to find the treatment functions ( $v_L$ ,  $v_M$  and  $v_A$ ) for the most commonly used treatment schedules. In Sections 6.2 and 6.3, we will also use other dosing schedules, which will be calculated in the same way. Unless otherwise noted, the treatment regimens have been adapted from De Vita's book titled *Cancer: Principles and Practice of Oncology* (2000).

### 5.9.1 Activated CD8<sup>+</sup>T-Cell Treatments

$v_L$  (IU/L/day) is unchanged from  $1.44 \times 10^{10}$  IU/L/day, the dose calculated by de Pillis and colleagues (2009). We would like to give this dose over 1 hour=0.04167 days (see Figure 5.5), so we want to set

$$v_L(t) = \begin{cases} 4.248 \times 10^{11} \text{ IU/L/day} & \text{if } t \in \{0, 0.04167\}, \\ 0 & \text{otherwise.} \end{cases}$$

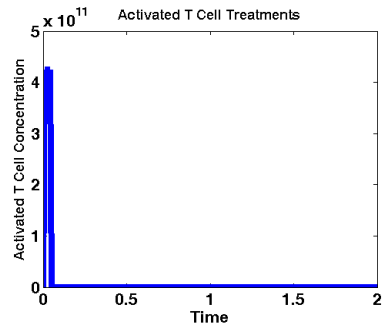


Figure 5.4: Activated  $CD8^+$ T-cell treatment, given only on the first day of treatment.

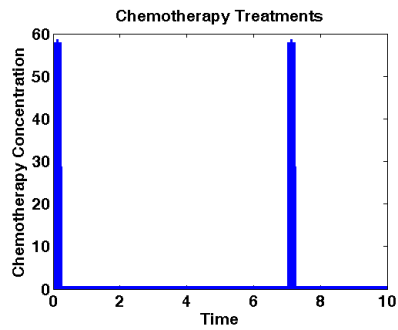


Figure 5.5: Irinotecan dosing schedule for the first 10 days of treatment. Note that spikes in medication level are slightly offset (by  $1/12$  days) from day 0 and 7.

### 5.9.2 Irinotecan Treatments

$v_M$  (mg/L/day) has been changed to fit a common treatment regimen for irinotecan. A 125 mg/m<sup>2</sup> dose of irinotecan is usually given over 90 minutes once weekly (see Figure 5.5). We assume that the course lasts for 6 weeks. Because the irinotecan molecule must be converted to an active form in the body before it can be used, the effect has a two-hour delay. We assume 1.73 m<sup>2</sup> to be the average surface area of an adult (Ratain, 1998). Because the medication quickly leaves the blood stream, we will use 59.71 L, the average volume of an adult, as the volume over which the medication is spread (de Pillis et al., 2009). So, we would like each dose to infuse

$$125 \frac{\text{mg}}{\text{m}^2} \times 1.73 \text{ m}^2 \times (59.71 \text{ L})^{-1} = 3.6217 \text{ mg/L},$$

and because it will be given over 90 minutes=0.0625 days, we want to set

$$v_M(t) = \begin{cases} 57.947 \text{ mg/L/day} & \text{if treatment was given at time } (t - 2/24), \\ 0 & \text{otherwise.} \end{cases}$$

We check for treatments at time  $(t - 2/24)$  because irinotecan needs to be converted by the body to its active form, SN-38, and SN-38 levels reach their peak two hours after irinotecan levels (De Vita, Jr et al., 2000).

### 5.9.3 Cetuximab Treatments

For cetuximab, a loading dose of 400 mg/m<sup>2</sup> is usually given over two hours, followed by a weekly 250 mg/m<sup>2</sup> dose over 60 minutes (see Figure 5.6(a)). Cetuximab is given on a six-week periodic schedule, during which it is given weekly for the first four weeks, then not given for two weeks. We will assume the same surface area and volume as in Section 5.6. For the loading dose, we would like to infuse

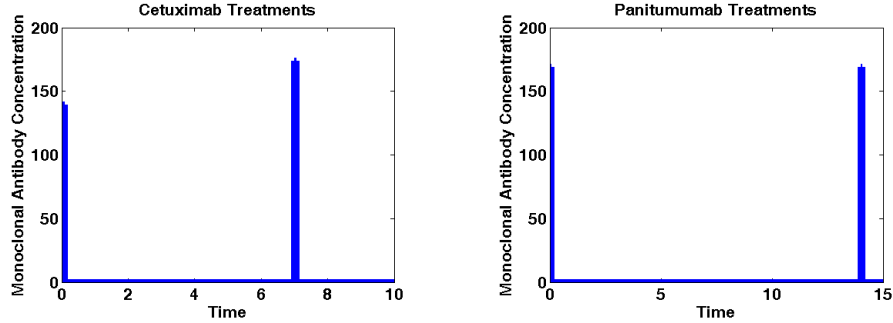
$$400 \frac{\text{mg}}{\text{m}^2} \times 1.73 \text{ m}^2 \times (59.71 \text{ L})^{-1} = 11.59 \text{ mg/L},$$

and because it will be given over two hours=0.0833 days, we want to set

$$v_A(t) = \frac{11.59 \text{ mg/L}}{0.0833 \text{ days}} = 139.072$$

for the first two hours of the simulations. For the regular weekly treatments, we would like to infuse

$$250 \frac{\text{mg}}{\text{m}^2} \times 1.73 \text{ m}^2 \times (59.71 \text{ L})^{-1} = 7.243 \text{ mg/L},$$



(a) Cetuximab dosing schedule for the first 10 days of treatment. Note the different size of the initial loading dose.

(b) Panitumumab dosing schedule during the first 15 days of treatment.

Figure 5.6: Monoclonal antibody dosing schedules.

and because it will be given over 60 minutes=0.04167 days, we want to set

$$v_A(t) = \frac{7.243 \text{ mg/L}}{0.04167 \text{ days}} = 173.840.$$

Thus, at any time  $t$ ,

$$v_A(t) = \begin{cases} 139.072 \text{ mg/L/day} & \text{if } t \in (0, \frac{2}{24}) \\ 173.840 \text{ mg/L/day} & \text{if treatment was given at time } t \text{ \& } t \geq \frac{2}{24} \\ 0 & \text{if treatment was not given at time } t. \end{cases}$$

#### 5.9.4 Panitumumab Treatments

The value of  $v_A$  for panitumumab was found in the same way, except that panitumumab does not require a loading dose (Figure 5.6(b)). We assume a treatment regimen of 6 mg/kg every two weeks, for a total of three treatments. We assume that the medication is given over 60 minutes, and that an average adult weighs of 70 kg (Lewis, 2009). This gives us

$$v_A(t) = \begin{cases} 168.816 \text{ mg/L/day} & \text{if treatment was given at time } t \\ 0 & \text{if treatment was not given at time } t. \end{cases}$$

## Chapter 6

# Results and Analysis

In our simulations, we use the initial conditions discussed in Section 5.1.3:

$$N = 9 \times 10^7, L = 5 \times 10^4, C = 10^9, M = 0, I = 1173, A = 0,$$

and we fix our initial tumor size at  $T = 10^9$  cells. Most of the tumors being treated with MAB therapy have already been growing for a long time, so we expect them to initially be large. However, we also wanted allow for the tumors to continue growing in our simulations. Thus, we chose a convenient initial tumor size that is about 20-25 percent of the carrying capacity.

In Sections 6.1, 6.2, and 6.3, we fix the patient-specific parameters  $d$ ,  $l$ , and  $s$  at  $d = 1.9$ ,  $l = 1.6$ , and  $s = 7 \times 10^{-3}$  to make it possible to plot sample results. For these plots of a single patient receiving one course of medication, we set  $K_T$  and  $\psi$  to values at both the low and high end of their ranges. This allows us to more easily show the range of possible results, and to know what response strength our plot represents. Each tumor (and therefore each patient) has only one value for each of  $K_T$  and  $\psi$ , so the simulations that result from setting these parameters are possible plots that can be generated when the values are generated randomly; setting  $K_T$  and  $\psi$  only speeds up the process of getting varied results. The importance of allowing  $K_T$  and  $\psi$  to vary arises in our simulations of clinical trials with our 64 different patients, because the tumors of each of these patients will respond differently to the medications due to the properties of the tumor, separate from the properties of the patient's immune system.

We use three values for  $K_T$  and  $\psi$ : 10 percent of the maximum response to represent a weak response, 75 percent of the maximum response (the expected value of the variables) to represent a moderate response, and 100 percent of the maximum response to represent a strong response.

## 6.1 Current Monotherapies

We plotted irinotecan, cetuximab, and panitumumab as monotherapies, for tumors with either a weak or strong reaction to the medication. For irinotecan, we can see that if the tumor has a weak response to irinotecan it will quickly grow. If the tumor has a strong response to the medication, it will grow slightly, but while growing will exhibit a strong oscillation in cell count, corresponding to treatments (see Figure 6.1).

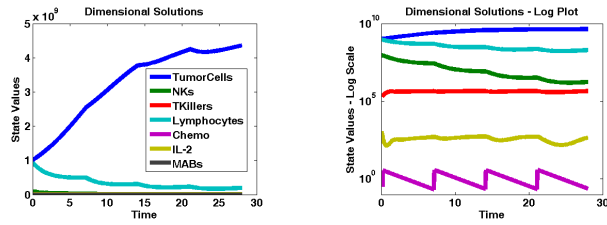
Similarly, we see that if the tumor has a weak response to cetuximab it will quickly grow. If the tumor has a strong response to the medication, it will again grow slightly, but while growing will exhibit a strong oscillation in cell count, corresponding to treatments (see Figure 6.2). For panitumumab, we see tumor growth similar to growth with cetuximab treatments, for both a strong and weak response (see Figure 6.3).

## 6.2 Current Combination Treatments

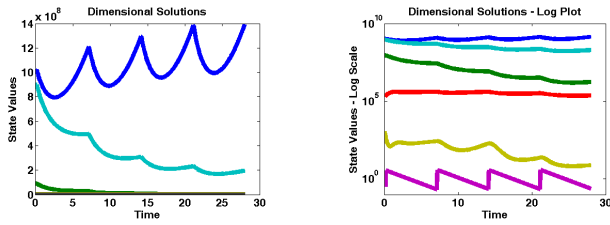
We plotted combination therapies of irinotecan, cetuximab or panitumumab, and activated CD8<sup>+</sup>T-cell treatments for tumors with either a weak or strong reaction to chemotherapy and, separately, MAB therapy. When a tumor does not respond strongly to either treatment, the tumor will quickly grow to the carrying capacity (see Figure 6.4).

When the tumor responds weakly to one of the medications but strongly to the other, the tumor does not grow as quickly as when it has a weak response to both medications, but we are still unable to eradicate the tumor completely (see Figure 6.5).

When the tumor responds strongly to both medications, we see that for this set of patient-specific parameters,  $d = 1.9$ ,  $l = 1.6$ ,  $s = 7 \times 10^{-3}$ , a cetuximab/irinotecan combination treatment and a panitumumab/irinotecan combination treatment are both able to significantly shrink the tumor (see Figure 6.6), but neither can eradicate it completely. However, for patient-specific parameters representing a patient with a slightly stronger immune system (recall from Section 5.2 that a stronger immune system is indicated by a low  $l$  and  $s$  and a high value for  $d$ ), these treatment combinations can eradicate the tumor. For example, if we set  $l = 1.3$  instead of 1.6 and  $s = 4 \times 10^{-3}$  instead of  $7 \times 10^{-3}$  while leaving all other parameters and starting values the same, the cetuximab/irinotecan combination treatment (see Figure 6.7(a)) and the panitumumab/irinotecan combination treatment (see

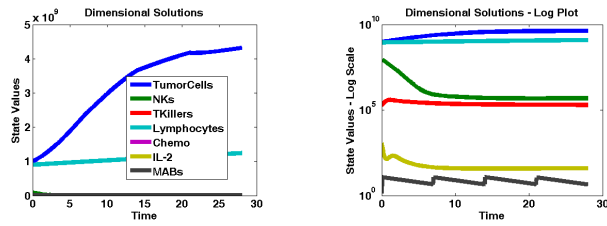


(a) Linear plot and log plot of a weak tumor response.

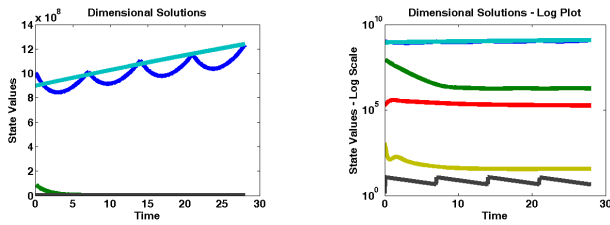


(b) Linear plot and log plot of a strong tumor response.

Figure 6.1: Tumor response to irinotecan monotherapies.

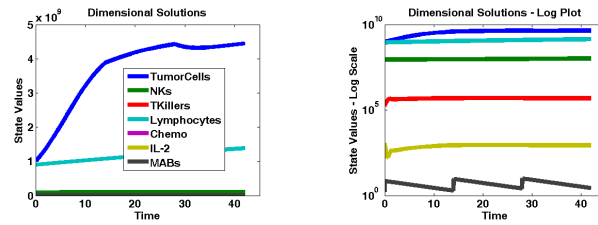


(a) Linear plot and log plot of a weak tumor response.

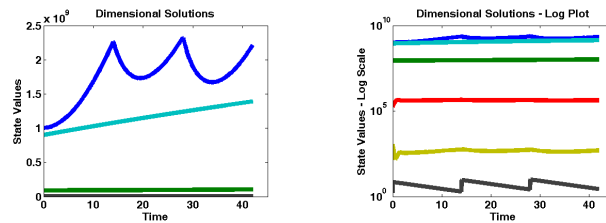


(b) Linear plot and log plot of a strong tumor response.

Figure 6.2: Tumor response to cetuximab monotherapies.



(a) Linear plot and log plot of a weak tumor response.

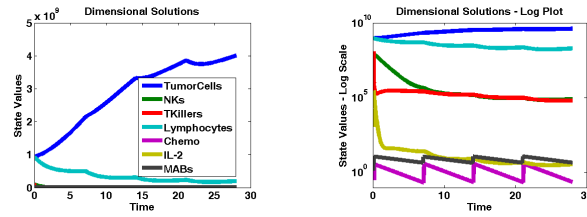


(b) Linear plot and log plot of a strong tumor response.

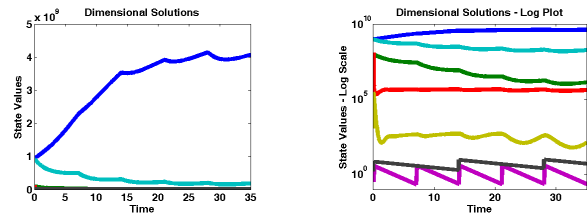
Figure 6.3: Tumor response to panitumumab monotherapies.

Figure 6.7(b)) both successfully reduce tumor size enough that the tumor approaches the *no tumor equilibrium* (see Figure 6.7(a)).

With our model, we can also simulate clinical trials with multiple patients and examine the overall response rates. For the most common treatment regimens, using the  $v_L$ ,  $v_M$ , and  $v_A$  calculated in Section 5.9, we found the response rates shown in Table 6.1. Our response rates are separated into “Partial Response”, meaning the tumor shrank but was not eradicated, and “Complete Response”, meaning the tumor was reduced enough to be attracted to the *no tumor equilibrium*. For monotherapies, our response rates match those of clinical trials very closely. For combination therapies, the responses from our model one week after the first treatment ended were much stronger than those seen in clinical trials. However, clinical trials are not consistent in the number of days between trial completion and determining the effect of the medication. If we measure the response rates for our simulations after seven weeks, when patients have had a few weeks of no treatment and doctors are likely to be evaluating whether or not to continue with an additional treatment course, we end up with response rates very similar to those found in clinical trials. After seven weeks, our patients on cetuximab/irinotecan have an overall response rate of 16 percent, and our patients on panitumumab/irinotecan have a response rate of 21 percent.

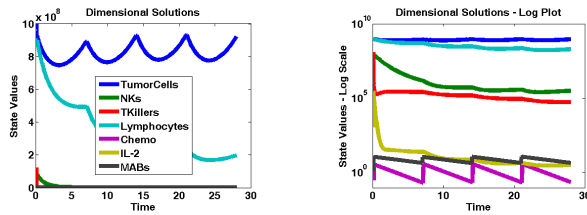


(a) Linear plot and log plot of a weak tumor response to irinotecan and cetuximab.

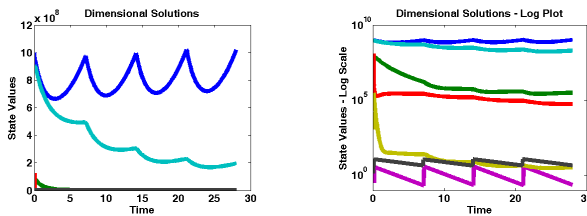


(b) Linear plot and log plot of a weak tumor response to irinotecan and panitumumab.

Figure 6.4: Weak tumor response to irinotecan and MABs in combination therapy.

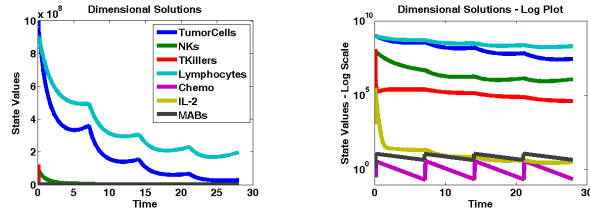


(a) Linear plot and log plot of a weak tumor response to irinotecan and a strong response to cetuximab.

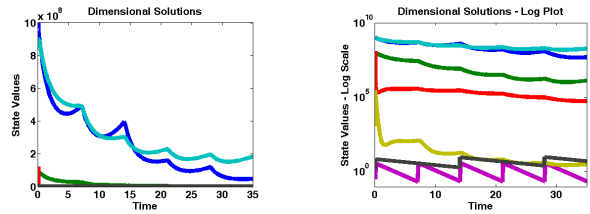


(b) Linear plot and log plot of a strong tumor response to irinotecan and a weak response to cetuximab.

Figure 6.5: Strong tumor response to only one medication in combination therapy with cetuximab.

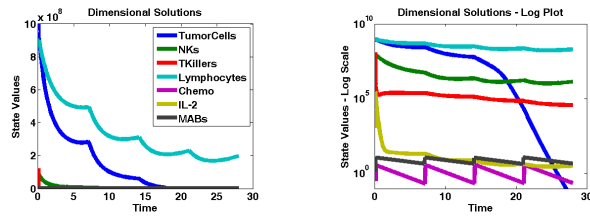


(a) Linear plot and log plot of a strong tumor response to irinotecan and to cetuximab.

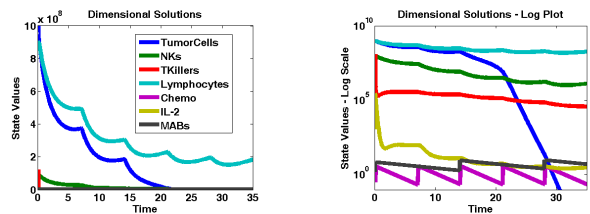


(b) Linear plot and log plot of a strong tumor response to irinotecan and to panitumumab.

Figure 6.6: Strong tumor response to irinotecan and MABs in combination therapy.



(a) Linear plot and log plot of response to cetuximab and irinotecan.



(b) Linear plot and log plot of response to panitumumab and irinotecan.

Figure 6.7: Strong tumor response to the medications, with  $l = 1.3$  and  $s = 4 \times 10^{-3}$ .

Medication <sup>a</sup>			Our Results			Published Results			Source
Name	Dose	Freq.	N	PR	CR	N	PR	CR	
Irinotecan	125 mg/m <sup>2</sup>	q1w	320	6.9%	1.3%	none <sup>b</sup>			
Cmab	400 mg/m <sup>2</sup> 250 mg/m <sup>2</sup>	load & q1w	320	10.0%	<1%	NP	9-11%	NP	De Vita, Jr et al. (2000)
			346			11.6%	NP	Lenz (2007)	
			111			10.8%	0%	Cunningham et al. (2004)	
Pmab	6 mg/kg	q2w	320	13.1%	<1%	NP	13%	NP	De Vita, Jr et al. (2000)
			231			10%	NP	Gravalos et al. (2009)	
Irinotecan and Cmab	125 mg/m <sup>2</sup> 400 mg/m <sup>2</sup> 250 mg/m <sup>2</sup>	q1w, load, q1w	320 <sup>d</sup>	68.4%	10.9%	NP	22.5-9%	NP	De Vita, Jr et al. (2000)
			320	5%	10.9%	NP	23%	NP	Grothey (2006)
			NP			22.9%	0%	Cunningham et al. (2004) <sup>c</sup>	
Irinotecan and Cmab	350 mg/m <sup>2</sup> 400 mg/m <sup>2</sup> 250 mg/m <sup>2</sup>	q3w, load, q1w	320	64.4%	17.5%	648	15%	1.4%	Sobrero et al. (2008)
Irinotecan and Pmab	125 mg/m <sup>2</sup> 6 mg/kg	q1w, q2w	320 <sup>d</sup>	56.0%	10.6%	34	20%	NP	Gravalos et al. (2009) <sup>c</sup>
			320	9.1%	11.9%				

Table 6.1: Response rates to common treatment schedules.

<sup>a</sup>Abbreviations: Pmab=panitumumab; Cmab=cetuximab; q1w=every week; q2w=every two weeks; q3w=every three weeks; load=loading dose; N=number of patients; PR=partial response; CR=complete response; NP=not provided.

<sup>b</sup>Most response rates for irinotecan found in the literature are for irinotecan as a first-line treatment. However, patients receiving MAB therapy are usually receiving it because they did not respond well to chemotherapy (Cunningham et al., 2004).

<sup>c</sup>Irinotecan dosing schedule was varied during the study.

<sup>d</sup>The first response rates (RRs) are measured 7 days after completion of first treatment. The second RRs for each are measured 7 weeks after treatment began.

### 6.3 Tumor Growth With Experimental Treatments

Since the responses of our combination therapies in the model are stronger than the results we see in clinical trials, we will compare the results of experimental treatments to those of the treatment schedules found in Section 5.9. This results in one treatment schedule each for panitumumab/irinotecan and cetuximab/irinotecan, which will be referred to in this section as the “standard treatments”. For each experimental treatment tested, we first looked at whether it increased or decreased final tumor size from the response to the standard treatments. Since we wanted to see the change in response of one patient’s tumor under each treatment, we fixed the patient-specific parameters to those given in Section 6 and  $K_T$  and  $\psi$  to 75 percent strength. Once treatments were identified which reduced final tumor size, we ran a clinical trial simulation on the treatment, and compared the responses to those of the standard treatment.

We currently do not have “patient health” (e.g., quality of life, negative side effects of the drugs, inconvenience of treatments) built into the model, so we used lymphocyte count to determine whether a treatment is valid. Grade 4 leukopenia, which indicates the worst depletion of leukocytes, is considered to be any leukocyte count below  $1 \times 10^9$  cells/L (Welink et al., 1999). We use 16 percent, the low end of the range for percent of leukocytes that are classified as lymphocytes, as reported in Section 5.5, and consider only the 90 percent of those lymphocytes which are not NK cells or CD8<sup>+</sup>T cells. This gives us  $1.44 \times 10^8$  as the lowest possible value for  $C$  that avoids grade four leukopenia, so any treatments resulting in a lymphocyte count below this number for any patient are considered invalid.

We have found two treatment schedules for each medication that give improved results over the standard treatments (see Table 6.2). For the first, we left the doses and administrating frequencies the same, but begin the cetuximab and panitumumab treatments four days after the cetuximab treatments. Interestingly, although starting the MAB treatment 4 days late was an improvement, beginning the chemotherapy 4 days after the MAB treatments gave a slightly worse outcome (<1 percent increase in final tumor size for cetuximab, 2 percent increase in final tumor size for panitumumab). For cetuximab, we saw only a small decrease in tumor size of approximately 1 percent, and only a slight increase of an additional 6 percent of patients had a partial response in the clinical trial simulation (see Figure 6.8). For panitumumab, we saw a 19 percent decrease in final tumor size, and an additional 14 percent of patients had a partial response to the medication, but again no increase in patients with a complete response (see Figure 6.9).

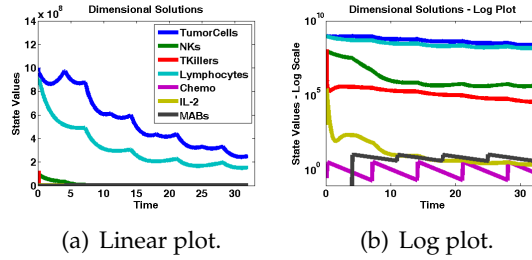


Figure 6.8: Cetuximab treatments started at  $t = 4$  days.

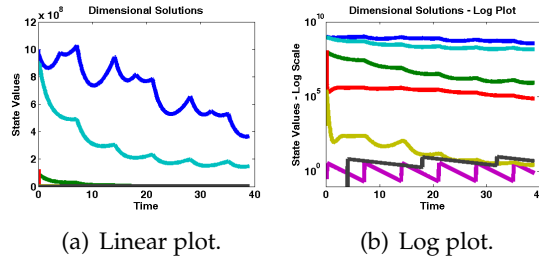


Figure 6.9: Panitumumab treatments started at  $t = 4$  days.

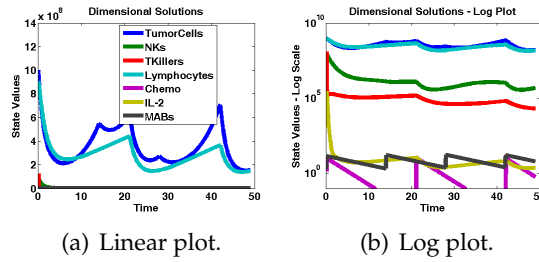


Figure 6.10: High dose irinotecan and cetuximab treatments.

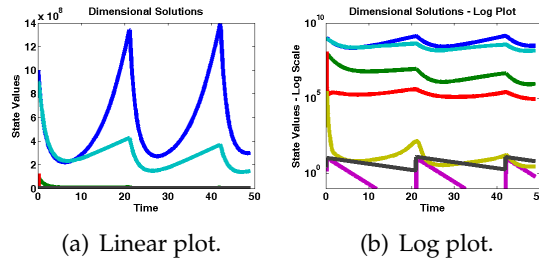


Figure 6.11: High dose irinotecan and panitumumab treatments.

Medication			Our Results <sup>a</sup>		
Name <sup>b</sup>	Dose	Frequency <sup>c</sup>	N	PR	CR
Irinotecan <sup>d</sup> and Cmab	125 mg/m <sup>2</sup> 400 mg/m <sup>2</sup> 250 mg/m <sup>2</sup>	weekly, load & weekly	320	68.44%	10.94%
Irinotecan <sup>d</sup> and Pmab	125 mg/m <sup>2</sup> 6 mg/kg	weekly & q2w	320	56.00%	10.63%
Irinotecan and Cmab	125 mg/m <sup>2</sup> 400 mg/m <sup>2</sup> 250 mg/m <sup>2</sup>	weekly & load, day 4 & weekly	320	74.06%	10.94%
Irinotecan and Pmab	125 mg/m <sup>2</sup> 6 mg/kg	weekly & q2w, day 4	320	70.99%	10.31%
Irinotecan and Cmab and Pmab	350 mg/m <sup>2</sup> 350 mg/m <sup>2</sup> 9 mg/kg	q3w q2w q3w	320	52.19%	37.5%

<sup>a</sup>N=number of patients; PR=partial response; CR=complete response.

<sup>b</sup>Pmab=panitumumab; Cmab=cetuximab

<sup>c</sup>q3w=every three weeks; q2w=every two weeks; load=loading dose.

<sup>d</sup>The standard treatments.

Table 6.2: Response rates to our experimental treatment schedules.

The second improved treatment schedule gives patients a high dose of both medications given less frequently. The high dose treatments have been used occasionally as a monotherapy, but to our knowledge have not been combined. Irinotecan can be given as a dose of 350 mg/m<sup>2</sup> every three weeks without additional side effects for the patient, so we use this as our irinotecan dose Sobrero et al. (2008); Lenz (2007). We first combined this with a high dosing schedule for cetuximab of 350 mg/m<sup>2</sup> every other week (Lenz, 2007). This dosing schedule resulted in a decrease in final tumor size of 39 percent from the standard treatment, and an additional 25 percent of the patients had a complete response to the treatment (see Figure 6.10). We next combined the high irinotecan dose with a 9 mg/kg dose given every 3 weeks (Gravalos et al., 2009). This dosing schedule results in a decrease in final tumor size of 34 percent from the standard treatment,

and an additional 7 percent of the patients had a complete response to the treatment (see Figure 6.11).

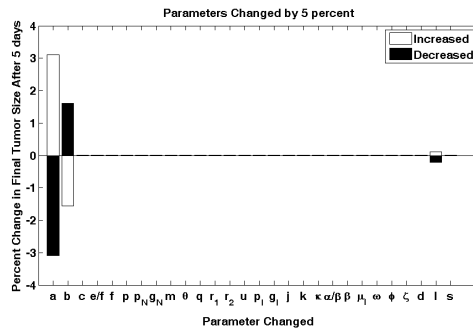
## 6.4 Sensitivity to Parameters

Parameter sensitivity analysis was performed to determine which model parameters have the biggest effect on final tumor size. First, sensitivity to non medication parameters was examined in simulations with no medication given. Each parameter value was increased and decreased by 5 percent, and the tumor size was measured at 5 days and 20 days, at which times the tumor is still growing very quickly and is close to its maximum volume, respectively, in our model (see Figure 6.12). Note that, while  $b$  (which, unsurprisingly, represents the inverse of the carrying capacity) is by far the most important parameter in determining final tumor size,  $a$  (the exponential tumor growth rate) plays a much more important role in determining how quickly the tumor reaches its maximum volume. The parameter  $l$ , an immune system scaling factor, is also important in determining the tumor growth rate.

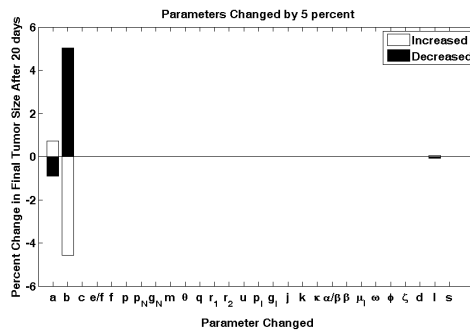
The sensitivity of the model to the MAB parameters was also examined. For both cetuximab and panitumumab, the final tumor size was found to be sensitive to  $\psi$ , the strength of the tumor's response to MAB drugs, and to  $\eta$ , the MAB turnover rate (see Figures 6.13 and 6.14). This is expected, since the main anti-tumor activity of MAB medications is through interference with the ability of EGF to bind to EGFR on the tumor cell surface, an activity which is included in the term  $\psi$  (De Vita, Jr et al., 2000). Short term, cetuximab also shows some sensitivity to  $\zeta$  and  $p_A$ , which are the parameters that determine the strength of ADCC activity (see Figure 6.13(a)).

We also checked the sensitivity of the model to the chemotherapy parameters. The final tumor size was found to be very sensitive to  $K_T$  and  $\delta_T$ , which determine the model's response to chemotherapy, and  $\gamma$ , which represents the excretion of the chemotherapy drug (see Figure 6.15). The size of the peak in tumor volume between treatments was much more dependent on  $\gamma$  than the size of the nadir after treatments. This makes sense, because if the chemotherapy is able to last longer in the body, it will be more effective at maintaining lower tumor volumes between treatments.

Finally, we also checked the sensitivity of the model to the parameter  $K_{TA}$ , which represents the increase in effectiveness of chemotherapy when it is used in conjunction with MAB therapy. With a 5 percent increase and decrease in the value of  $K_{TA}$ , the final tumor size after 28 days changed by less than 0.5 percent (figure not shown).

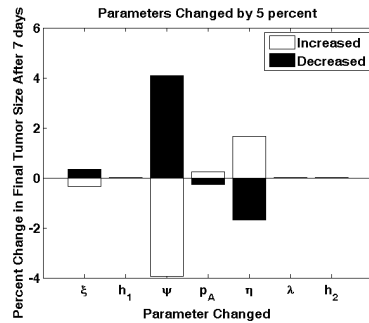


(a) Final tumor size measured at 5 days.

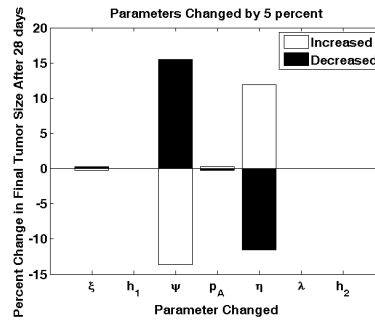


(b) Final tumor size measured at 20 days.

Figure 6.12: Sensitivity of final tumor size to a 5% change in non-medication parameters.



(a) Change in tumor growth after 7 days.



(b) Change in tumor growth after 28 days.

Figure 6.13: Sensitivity of final tumor size to a 5% change in cetuximab parameters.

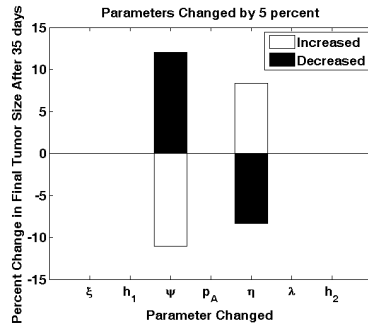
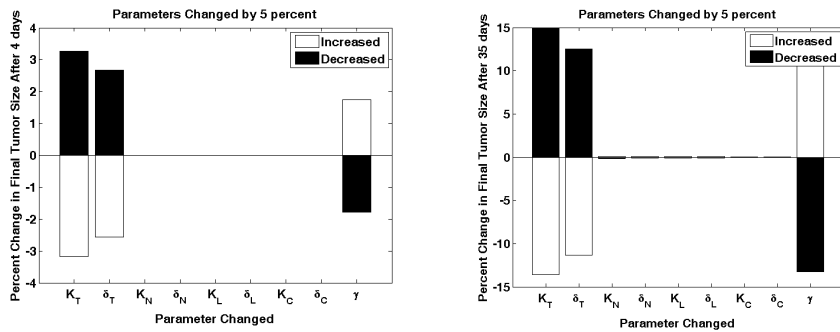


Figure 6.14: Sensitivity of final tumor size to a 5% change in panitumumab parameters after 35 days.



(a) Change in tumor growth after 4 days.

(b) Change in tumor growth after 35 days.

Figure 6.15: Sensitivity of final tumor size to a 5% change in irinotecan parameters.



## Chapter 7

# Discussion

We have edited the model of de Pillis and colleagues (2009) to include monoclonal antibody treatment, and we have found, calculated, or estimated parameter values to make the model specific for colorectal cancer, the chemotherapy treatment irinotecan, and the monoclonal antibodies cetuximab and panitumumab. We have found two separate stable equilibrium states, a *no tumor equilibrium* and a *large tumor equilibrium*, and seen that tumors can be driven to either of these states, depending on the patient's immune system and the treatments given. We have also added two parameters that are constant for each patient (within each individual simulation run), but can be randomly generated for each tumor at the beginning of the simulation. These parameters,  $K_T$  and  $\psi$ , represent the range of different tumor responses to the same chemotherapy and MAB treatments. Colorectal tumors can have a wide variety of mutations, and some of these mutations limit the medication's ability to function correctly. Besides making biological sense, these randomly chosen variables helped us to achieve the results seen in clinical trials.

When our model is run over our set of 64 "patients," our model matches clinical trials for monotherapy very well. For combination therapies, our tumor population seems to often be too response to the medication, however this could likely be fixed if more work was done on choosing a more accurate way to model the variance in tumor responses. Also, if response rates are measured a few weeks after the treatments have finished, which might be done if tumor size is measured to determine additional treatments instead of to measure the effectiveness of the previous medication, then our results match the results of the clinical trials very closely. We find a 16 percent response rate for cetuximab/irinotecan, compared to 22 percent

response rate found in clinical trials (De Vita, Jr et al., 2000), and a 21 percent response rate for panitumumab/irinotecan, compared to a 20 percent response rate found in clinical trials (Gravalos et al., 2009). However, for panitumumab/irinotecan combination therapies, very few clinical trial results are available. Multiple clinical trial results are available for cetuximab, but many do not specify irinotecan dosing (or use a variety of doses), and many also do not specify whether the patient has received treatment previously, how long the treatment was given, and other useful information. We are confident that overall, our model gives a qualitatively good prediction of likely results for various dosing schedules.

Many of the combination treatments we experimented with, which used different doses, dosing frequencies, and different start times for each medication, were not as successful at shrinking the tumor as the current standard treatments. However, we did find two treatments which appear to provide a better outcome for the patients. One of these, which provided only minor improvements, required offsetting the MAB medication administration by 4 days from the chemotherapy. This treatment plan, which does not require a change in dose size or frequency, resulted in more patients with partial responses to the medications. This treatment plan may also help to reduce the strength of the negative side effects associated with each of these medications. However, it also requires the patient to receive treatment twice a week for at least an hour, and this inconvenience may offset the other potential benefits.

We also found a treatment option that combined a higher dose of the drugs administered less frequently. This treatment option was very successful in our model, and particularly for the irinotecan/cetuximab treatment, allowed for many more patients to reach the *no tumor equilibrium*. The resulting lymphocyte count from this treatment was barely above the lymphocyte count that we considered to be unacceptably low ( $1.44 \times 10^8$  versus  $1.47 \times 10^8$ ), so it is possible that in practice this particular treatment would be too harsh for the patient. However, variations on this treatment may be worth exploring in a clinical setting, especially if supportive care is available or the patient is starting out healthier than the patients we considered. Each of the three treatments (less frequent, high dose cetuximab, panitumumab, and irinotecan) individually causes large dips and spikes in tumor cell count, so one feature that was particularly useful about this cetuximab/irinotecan combination, compared to other cetuximab/irinotecan combinations that we looked at, was that the high dose cetuximab is given every two weeks, whereas the high dose irinotecan is given every three weeks, so the treatments are not always given at the same time and are able

---

to work together to keep the tumor population low. Neither giving panitumumab every two weeks nor offsetting the higher dose panitumumab to alternate weeks with the irinotecan had this same effect, although it's possible that a higher dose of panitumumab may be able to achieve this. A treatment schedule like this would also be convenient for the patient, because medication (and the negative side effects that come with it) would be required less frequently.

The parameter sensitivity did not provide any particularly surprising results, however it is useful to think about which parameters could be possible targets for reducing tumor size. For example, if we can get a better sense of biologically how to influence  $l$ , a large decrease in  $l$  would result in an immune system that is able to conquer the tumor much more easily than a change in the other immune system parameters.

In the future, it would be very helpful to make two important changes to the model. First, it would be helpful to tailor the parameters  $K_T$  and  $\psi$  to have a more specific biological meaning. For example, the KRAS mutation is known to be present in about 40 percent of all colorectal tumors, and is known to reduce the effectiveness of MAB treatment to almost zero (De Roock et al., 2008; Amado et al., 2008). Collecting information on how factors such as whether the tumor is a KRAS mutant and the EGRF counts on the tumor cells could allow for these parameters to be chosen from a small distribution based on features of the tumors cells, instead of from a larger random distribution. Also, an equation representing patient well-being would be very useful for predicting effective treatments. Although using lymphocyte count allows us to determine that the patient's immune system has not been completely destroyed by the medication, it doesn't take into account factors such as that frequent treatments may be inconvenient or that high doses of medication also results in stronger harmful side effects.



# Appendix A

## Biology Glossary

Unless otherwise stated, all definitions are from Sompayrac's *How the Immune System Works* (2008).

**Adaptive immune system** The part of our immune system that is targeted for a specific invader. It is slow to activate but an effective killer.

**Antibody** Proteins that help the adaptive immune system by targeting a particular invader and then helping the NK cells to find it.

**Antibody-dependent cellular cytotoxicity** Antibody-directed killing of tumor cells by natural killer cells. The antibodies activate the NK cells and direct connect them to their target.

**Antigen** The target of an antibody's or T cell's search, such as a protein on an invading cell.

**Apoptosis** The process during which a cell commits suicide, either due to problems within the cell or signals from another cell.

**B cell** Lymphocytes that can produce antibodies.

**Binding affinity** How tightly two molecules bind together. Can be represented by the dissociation constant (with units of molarity= $M=\text{mol/L}$ ), which is the concentrations of the separate molecules divided by the concentrations of the complexes, so a smaller dissociate constant means that the molecules bind together more tightly (Voet et al., 2008).

**Chemotherapy** Chemotherapeutic drugs kill off rapidly dividing cells (Sompayrac, 2004).

**Complement system** The complement system is a protein cascade that is activated when invaders are present. These proteins help to recruit other cells to kill the invaders. In some cases, they can also destroy invading cells themselves, as in complement-dependent cytotoxicity. Also called the complement cascade.

**Complete response** The disappearance of all signs of cancer in response to treatment (National Cancer Institute, 2010).

**Cytokines** Messenger molecules that cells use to communicate.

**Dendritic cell** Leukocytes that present antigens to T cells to let them know what to target.

**Epidermal growth factor** A protein made in the body with causes cells to grow and mature. It is a type of cytokine (National Cancer Institute, 2010).

**Epidermal growth factor receptor** A protein found on the surface of some cells, to which the epidermal growth factor binds to cause cell proliferation. It is found in abnormally high levels on many types of cancer cells (National Cancer Institute, 2010).

**Extracellular domain** The part of a receptor that sticks out of the cell (National Cancer Institute, 2010).

**Homeostasis** A steady state condition in the body, in which concentrations are remaining constant (Voet et al., 2008).

**Innate immune system** The part of our immune system which is always prepared to fight invaders, without activation.

**Interleukin-2** A cytokine that is used as communication between leukocytes.

**In vitro** A study conducted in a controlled (lab) environment, usually in cultured cells (Voet et al., 2008).

**In vivo** A study conducted in a living organism, usually referring to animal testing or clinical trials (Voet et al., 2008).

**Leukocyte** White blood cells, the cells that make up our immune system.

**Lymphocyte** One type of leukocyte, make up to T cells and B cells

**Metastasize** When tumors have metastasized, it means that the tumor cells have spread to new locations in the body and have begun to grow new tumors.

**MHC proteins** The presence of the proper MHC proteins on the surfaces of our cells helps other molecules know which cells are invaders and which belong.

**Monoclonal antibody** Antibodies that are manufactured specifically to target cancer cells, by binding to proteins on the cells' surfaces (Sompayrac, 2004).

**Natural killer cell** A type of lymphocyte that is part of both the innate and adaptive immune system. NK cells can be activated by cytokines or antibodies, and induce apoptosis in foreign cells.

**Partial response** A decrease in the size of the tumor in response to treatment (National Cancer Institute, 2010).

**Polyp** When the cells in the colon are mutated and proliferate too quickly, they form a mass of cells called a polyp. Only about 1 percent of polyps become metastatic cancer (Sompayrac, 2004).

**Professional phagocyte** Leukocytes that are part of the innate immune system. These cells engulf invaders.

**Proliferate** To divide/reproduce/increase in number.

**Receptor** Proteins on the surface of cells which bind to specific molecules, usually to send a signal to the cell.

**Response rate** Percentage of patients whose tumors respond to the treatment (National Cancer Institute, 2010).

**T cell** Lymphocytes with receptors that each recognize a specific antigen, which it is their job to find and kill. There are many kinds of T cells, such as the cytotoxic T cells, which are ready to kill invaders, and the helper T cells, which are important in directing cells to the invaders.

**Upregulation** The overproduction of a molecule, such as the upregulation of growth factor receptors on tumor cells (National Cancer Institute, 2010).



# Appendix B

## Reference Tables

### B.1 Equation Term Descriptions

Equation	Term	Description
$\frac{dT}{dt}$	$aT(1 - bT)$	Logistic tumor growth
	$-cNT$	NK-induced tumor death
	$-\zeta \frac{A}{h_1+A} NT$	MAB-induced tumor death from NK cell interactions
	$-DT$	CD8 <sup>+</sup> T cell-induced tumor death
	$-K_T(1 - e^{-\delta_T M})T$	Chemotherapy-induced tumor death
	$-K_{AT}A(1 - e^{-\delta_T M})T$	MAB-induced tumor death from increase in chemotherapy effectiveness
	$-\psi AT$	MAB-induced tumor death
$\frac{dN}{dt}$	$eC$	Production of NK cells from circulating lymphocytes
	$-fN$	NK turnover
	$-pNT$	NK death by exhaustion of tumor-killing resources
	$-p_A \frac{A}{h_1+A} NT$	Additional NK death by exhaustion of tumor-killing resources from MAB interactions
	$\frac{p_N NI}{s_N + I}$	Stimulatory effect of IL-2 on NK cells

*Continued on next page*

Table B.1: Equation Descriptions.

Equation	Term	Description
	$-K_N(1 - e^{-\delta_N M})N$	Death of NK cells due to chemotherapy toxicity
$\frac{dL}{dt}$	$\frac{\theta mL}{\theta + I}$	CD8 <sup>+</sup> T-cell turnover
	$j \frac{T}{k+T} L$	CD8 <sup>+</sup> T-cell stimulation by CD8 <sup>+</sup> T cell-lysed tumor-cell debris
	$-qLT$	CD8 <sup>+</sup> T-cell death by exhaustion of tumor-killing resources
	$r_1 NT$	CD8 <sup>+</sup> T-cell stimulation by NK-lysed tumor-cell debris
	$r_2 CT$	Activation of native CD8 <sup>+</sup> T cells in the general lymphocyte population
	$-\frac{uL^2 CI}{\kappa + I}$	Breakdown of surplus CD8 <sup>+</sup> T cells in the presence of IL-2
	$-K_L(1 - e^{-\delta_L M})L$	Death of CD8 <sup>+</sup> T cells due to chemotherapy toxicity
	$\frac{p_I LI}{g_I + I}$	Stimulatory effect of IL-2 on CD8 <sup>+</sup> T cells
$\frac{dC}{dt}$	$\alpha$	Lymphocyte synthesis in bone marrow
	$-\beta C$	Lymphocyte turnover
	$-K_C(1 - e^{-\delta_C M})C$	Death of lymphocytes due to chemotherapy toxicity
$\frac{dM}{dt}$	$-\gamma M$	Excretion and elimination of chemotherapy
$\frac{dI}{dt}$	$-\mu_I I$	IL-2 turnover
	$\phi C$	Production of IL-2 due to naive CD8 <sup>+</sup> T cells and CD4 <sup>+</sup> T cells
	$\frac{\omega LI}{\zeta + I}$	Production of IL-2 from activated CD8 <sup>+</sup> T cells
$\frac{dA}{dt}$	$-\eta A$	Excretion and elimination of MABs
	$-\lambda T \frac{A}{h_2 + A}$	Loss of MABs due to tumor-MAB binding

Table B.1: Equation Descriptions.

## B.2 Parameter Descriptions

Equation	Parameter	Description
$\frac{dT}{dt}$	$a$	Growth rate of tumor
	$b$	Inverse of carrying capacity
	$c$	Rate of NK-induced tumor death
	$\xi$	Rate of NK-induced tumor death through ADCC
	$h_1$	Concentration of MABs for half-maximal increase in ADCC
	$K_T$	Rate of chemotherapy-induced tumor death
	$K_{AT}$	Additional chemotherapy-induced tumor death due to MABs
	$\delta_T$	Medicine efficacy coefficient
	$\psi$	Rate of MAB-induced tumor death
	$\frac{dN}{dt}$	$\frac{e}{f}$
$f$		Rate of NK cell turnover
$p$		Rate of NK cell death due to tumor interaction
$p_A$		Rate of NK cell death due to tumor-MAB complex interaction
$p_N$		Rate of IL-2 induced NK cell proliferation
$g_N$		Concentration of IL-2 for half-maximal NK cell proliferation
$K_N$		Rate of NK depletion from chemotherapy toxicity
$\delta_N$		Chemotherapy toxicity coefficient
$\frac{dL}{dt}$	$m$	Rate of activated CD8 <sup>+</sup> T-cell turnover
	$\theta$	Concentration of IL-2 to halve CD8 <sup>+</sup> T-cell turnover
	$q$	Rate of CD8 <sup>+</sup> T-cell death due to tumor interaction
	$r_1$	Rate of NK-lysed tumor cell debris activation of CD8 <sup>+</sup> T cells
	$r_2$	Rate of CD8 <sup>+</sup> T-cell production from circulating lymphocytes
	$p_I$	Rate of IL-2 induced CD8 <sup>+</sup> T-cell activation
	$g_I$	Concentration of IL-2 for half-maximal CD8 <sup>+</sup> T-cell activation
	$u$	CD8 <sup>+</sup> T-cell self-limitation feedback coefficient

*Continued on next page*

Table B.2: Parameter Descriptions.

Equation	Parameter	Description
	$\kappa$	Concentration of IL-2 to halve magnitude of CD8 <sup>+</sup> T-cell self-regulation
	$j$	Rate of CD8 <sup>+</sup> T-cell lysed tumor cell debris activation of CD8 <sup>+</sup> T cells
	$k$	Tumor size for half-maximal CD8 <sup>+</sup> T-lysed debris CD8 <sup>+</sup> T activation
	$K_L$	Rate of CD8 <sup>+</sup> T-cell depletion from chemotherapy toxicity
	$\delta_L$	Chemotherapy toxicity coefficient
$\frac{dC}{dt}$	$\frac{\alpha}{\beta}$	Ratio of rate of circulating lymphocyte production to turnover rate
	$\beta$	Rate of lymphocyte turnover
	$K_C$	Rate of lymphocyte depletion from chemotherapy toxicity
	$\delta_C$	Chemotherapy toxicity coefficient
$\frac{dM}{dt}$	$\gamma$	Rate of excretion and elimination of chemotherapy drug
$\frac{dI}{dt}$	$\mu_I$	Rate of excretion and elimination of IL-2
	$\omega$	Rate of IL-2 production from CD8 <sup>+</sup> T cells
	$\phi$	Rate of IL-2 production from CD4 <sup>+</sup> /naive CD8 <sup>+</sup> T cells
	$\zeta$	Concentration of IL-2 for half-maximal CD8 <sup>+</sup> T-cell IL-2 production
$\frac{dA}{dt}$	$\eta$	Rate of MAB turnover and excretion
	$\lambda$	Rate of MAB-tumor cell complex formation
	$h_2$	Concentration of MABs for half-maximal EGFR binding
$D$	$d$	Immune-system strength coefficient
	$l$	Immune-system strength scaling coefficient
	$s$	Value of $(\frac{l}{T})^l$ necessary for half-maximal CD8 <sup>+</sup> T-cell toxicity

Table B.2: Parameter Descriptions.

### B.3 Parameter Values

Equation	Parameter	Value	Units	Main Source	
$\frac{dT}{dt}$	$a$	$2.31 \times 10^{-1}$	Day <sup>-1</sup>	Corbett et al. (1975)	
	$b$	$2.146 \times 10^{-10}$	Cells <sup>-1</sup>	Leith et al. (1987)	
	$c$	$5.156 \times 10^{-14}$	L Cells <sup>-1</sup> Day <sup>-1</sup>	de Pillis et al. (2009)	
	$\xi$	$6.5 \times 10^{-10*}$	L Cells <sup>-1</sup> Day <sup>-1</sup>	Kurai et al. (2007)	
		0**	L Cells <sup>-1</sup> Day <sup>-1</sup>	Grothey (2006)	
	$h_1$	$1.25 \times 10^{-6*}$	mg L <sup>-1</sup>	Kurai et al. (2007)	
		0**	mg L <sup>-1</sup>	Grothey (2006)	
	$K_T$	$0 - 8.1 \times 10^{-1}$	Day <sup>-1</sup>	Vilar et al. (2006)	
	$K_{AT}$	$4 \times 10^{-4*}$	L mg <sup>-1</sup> Day <sup>-1</sup>	<i>ad hoc</i> value	
		$4 \times 10^{-4**}$	L mg <sup>-1</sup> Day <sup>-1</sup>	<i>ad hoc</i> value	
	$\delta_T$	$2 \times 10^{-1}$	L mg <sup>-1</sup>	Vilar et al. (2006)	
	$\psi$	$0 - 2.28 \times 10^{-2*}$	L mg <sup>-1</sup> Day <sup>-1</sup>	De Vita, Jr et al. (2000)	
		$0 - 2.58 \times 10^{-2**}$	L mg <sup>-1</sup> Day <sup>-1</sup>	De Vita, Jr et al. (2000)	
	$\frac{dN}{dt}$	$\frac{e}{f}$	$\frac{1}{9}$	–	de Pillis et al. (2009)
		$f$	$1 \times 10^{-2}$	Day <sup>-1</sup>	Modified from de Pillis et al. (2009)
$p$		$5.156 \times 10^{-14}$	L Cells <sup>-1</sup> Day <sup>-1</sup>	de Pillis et al. (2009)	
$p_A$		$6.5 \times 10^{-10*}$	L Cells <sup>-1</sup> Day <sup>-1</sup>	Kurai et al. (2007)	
		0**	L Cells <sup>-1</sup> Day <sup>-1</sup>	Grothey (2006)	
$p_N$		$5.13 \times 10^{-2}$	Day <sup>-1</sup>	de Pillis et al. (2009)	
$g_N$		$2.5036 \times 10^5$	IU L <sup>-1</sup>	de Pillis et al. (2009)	
$K_N$		$9.048 \times 10^{-1}$	Day <sup>-1</sup>	Catimel et al. (1995)	
$\delta_N$		$2 \times 10^{-1}$	L mg <sup>-1</sup>	Vilar et al. (2006)	
$\frac{dL}{dt}$		$m$	$5 \times 10^{-3}$	Day <sup>-1</sup>	Modified from de Pillis et al. (2009)
	$\theta$	$2.5036 \times 10^{-3}$	IU L <sup>-1</sup>	de Pillis et al. (2009)	
	$q$	$5.156 \times 10^{-17}$	Cells <sup>-1</sup> Day <sup>-1</sup>	Modified from de Pillis et al. (2009)	
	$r_1$	$5.156 \times 10^{-12}$	Cells <sup>-1</sup> Day <sup>-1</sup>	de Pillis et al. (2009)	
	$r_2$	$1 \times 10^{-15}$	Cells <sup>-1</sup> Day <sup>-1</sup>	Modified from de Pillis et al. (2009)	
	$p_I$	2.4036	Day <sup>-1</sup>	de Pillis et al. (2009)	
	$g_I$	$2.5036 \times 10^3$	IU L <sup>-1</sup>	de Pillis et al. (2009)	

Continued on next page

Table B.3: Parameter Values.

Equation	Parameter	Value	Units	Main Source
	$u$	$3.1718 \times 10^{-14}$	$L^2 \text{Cells}^{-2} \text{Day}^{-1}$	de Pillis et al. (2009)
	$\kappa$	$2.5036 \times 10^3$	$IU L^{-1}$	de Pillis et al. (2009)
	$j$	$1.245 \times 10^{-4}$	$\text{Day}^{-1}$	Modified from de Pillis et al. (2009)
	$k$	$2.019 \times 10^7$	Cells	de Pillis et al. (2009)
	$K_L$	$4.524 \times 10^{-1}$	$\text{Day}^{-1}$	Catimel et al. (1995)
	$\delta_L$	$2 \times 10^{-1}$	$L \text{ mg}^{-1}$	Vilar et al. (2006)
$\frac{dC}{dt}$	$\frac{\alpha}{\beta}$	$3 \times 10^9$	$\text{Cells } L^{-1}$	InfoNet (2009)
	$\beta$	$6.3 \times 10^{-3}$	$\text{Day}^{-1}$	de Pillis et al. (2009)
	$K_C$	$5.7 \times 10^{-1}$	$\text{Day}^{-1}$	Catimel et al. (1995)
	$\delta_C$	$2 \times 10^{-1}$	$L \text{ mg}^{-1}$	Vilar et al. (2006)
$\frac{dM}{dt}$	$\gamma$	$4.077 \times 10^{-1}$	$\text{Day}^{-1}$	Catimel et al. (1995)
$\frac{dI}{dt}$	$\mu_I$	11.7427	$\text{Day}^{-1}$	de Pillis et al. (2009)
	$\omega$	$7.88 \times 10^{-2}$	$IU \text{ Cells}^{-1} \text{Day}^{-1}$	de Pillis et al. (2009)
	$\phi$	$1.788 \times 10^{-7}$	$IU \text{ Cells}^{-1} \text{Day}^{-1}$	de Pillis et al. (2009)
	$\zeta$	$2.5036 \times 10^3$	$IU L^{-1}$	de Pillis et al. (2009)
$\frac{dA}{dt}$	$\eta$	$1.386 \times 10^{-1*}$	$\text{Day}^{-1}$	Grothey (2006)
		$9.242 \times 10^{-2**}$	$\text{Day}^{-1}$	Grothey (2006)
	$\lambda$	$8.3 \times 10^{-14*}$	$\text{mg Cells}^{-1} L^{-1} \text{Day}^{-1}$	Freeman et al. (2008)
		$8.6 \times 10^{-14**}$	$\text{mg Cells}^{-1} L^{-1} \text{Day}^{-1}$	Freeman et al. (2008)
	$h_2$	$4.0 \times 10^{-5*}$	$\text{mg } L^{-1}$	Freeman et al. (2008)
$4.05 \times 10^{-5**}$		$\text{mg } L^{-1}$	Freeman et al. (2008)	
$D$	$d$	Not Specified	$\text{Day}^{-1}$	de Pillis et al. (2009)
	$l$	Not Specified	-	de Pillis et al. (2009)
	$s$	Not Specified	$L^{-1}$	de Pillis et al. (2009)

Table B.3: Parameter Values.

\*For cetuximab.

\*\*For panitumumab.

# Bibliography

Abbas, A.K., and A.H. Lichtman. 2005. *Cellular and Molecular Immunology*. Elsevier Saunders, 5th ed.

ACS. 2008. Colorectal cancer facts & figures 2008–2010. URL [http://www.cancer.org/docroot/STT/content/STT\\_1x\\_Colorectal\\_Cancer\\_Facts\\_\\_Figures\\_2008-2010.asp](http://www.cancer.org/docroot/STT/content/STT_1x_Colorectal_Cancer_Facts__Figures_2008-2010.asp).

Amado, R.G., M. Wolf, M. Peeters, Eric Van Cutsem, Salvatore Siena, Daniel J. Freeman, Todd Juan, Robert Sikorski, Sid Suggs, Robert Radinsky, Scott D. Patterson, and David D. Chang. 2008. Wild-type KRAS is required for panitumumab efficacy in patients with metastatic colorectal cancer. *J Clin Oncol* 26:1626–1634.

American Association for Cancer Research. 2010. AACR cancer concepts: HER2. URL <http://www.aacr.org/home/public--media/patients--family/fact-sheets/cancer-concepts/her2.aspx>.

Bhat, Rauf, and Carsten Watzl. 2007. Serial killing of tumor cells by human natural killer cells—enhancement by therapeutic antibodies. *PLoS ONE* 1–7.

Bolin, S., E. Nilsson, and R. Sjö Dahl. 1983. Carcinoma of the colon and rectum—growth rate. *Ann Surg* 198:151–158.

Burnett, Keith R., and Edward I. Greenbaum. 1981. Rapidly growing carcinoma of the colon. *Dis Colon Rectum* 24:282–286.

Catimel, G., G.G. Chabot, J.P. Guastalla, A. Dumortier, C. Cote, C. Engel, A. Gouyette, M. Mathieu-Boué, Mahjoubi, and M. Clavel. 1995. Phase I and pharmacokinetic study of irinotecan (CPT-11) administered daily for three consecutive days every three weeks in patients with advanced solid tumors. *Annals of Oncology* 6:133–140.

Chen, Z.Z., S.Y. Zhang, Q.S. Liu, P.F. Xiao, X.Y. Guo, and Z.H. Lu. 2005. Theoretical and experimental studies on filtering tumor cells from blood cell mixture with dam structure in microfluidic devices. *Engineering in Medicine and Biology 27th Annual Conference*.

Corbett, T.H., D.P. Griswold, Jr, B.J. Roberts, J.C. Peckham, and F.M. Schabel, Jr. 1975. Tumor induction relationships in development of transplantable cancers of the colon in mice for chemotherapy assays, with a note on carcinogen structure. *Cancer Research* 35:2434–2439.

Cunningham, D., Y. Humblet, and S. Siena. 2004. Cetuximab monotherapy and cetuximab plus irinotecan in irinotecan-refractory metastatic colorectal cancer. *N Engl J Med* 351:337–45.

de Pillis, Lisette, Renee Fister, Weiqing Gu, Craig Collins, Michael Daub, David Gross, James Moore, and Benjamin Preskill. 2009. Mathematical model creation for cancer chemo-immunotherapy. *Computational and Mathematical Models in Medicine* 1–19.

de Pillis, Lisette, Renee Fister, Weiqing Gu, Tiffany Head, Kenny Maples, Todd Neal, Anand Murugan, and Kenji Kozai. 2008. Optimal control of mixed immunotherapy and chemotherapy of tumors. *Journal of Biological Systems* 16:51–80.

de Pillis, Lisette, Ami Radunskaya, and Charles Wiseman. 2005. A validated mathematical model of cell-mediated immune response to tumor growth. *Cancer Research* 65.

De Roock, W., H. Piessevaux, J. De Schutter, M. Janssens, G. De Hertogh, N. Personeni, B. Biesmans, J.L. Van Laethem, M. Peeters, Y. Humblet, E. Van Cutsem, and S. Tejpar. 2008. KRAS wild-type state predicts survival and is associated to early radiological response in metastatic colorectal cancer treated with cetuximab. *Ann Oncol* 19:508–151.

De Vita, Vincent, Jr, Samuel Hellman, and Steven Rosenberg. 2000. *Cancer: Principles and Practice of Oncology*. Lippincott Williams & Wilkins, 7th ed.

Dharmananda, Subhuti. 2005. Deer antler to nourish blood, bone, and joints. URL <http://www.itmonline.org/arts/antler.htm>.

Eckert, K., E. Grünberg, P. Immenschuh, F. Garbin, E.D. Kreuser, and H.R. Maurer. 1997. Interleukin-2-activated killer cell activity in colorectal tumor patients: Evaluation of in vitro effects by prothymosin  $\alpha 1$ . *J Cancer Res Clin Oncol* 123:420–428.

- Freeman, D., J. Sun, R. Bass, K. Jung, S. Ogbagabriel, G. Elliot, and R. Radinsky. 2008. Panitumumab and cetuximab epitope mapping and in vitro activity. Poster: 2008 Gastrointestinal Cancers Symposium.
- Gatenby, Robert, and Thomas Vincent. 2003. Application of quantitative models from population biology and evolutionary game theory to tumor therapeutic strategies. *Molecular Cancer Therapeutics* 919–927.
- Goldberg, Richard, and Alfredo Carrato. 2008. Accomplishments in 2007 in the treatment of advanced colorectal cancer. *Gastrointestinal Cancer Research* 2:S19–S24.
- Gravalos, Christina, Javier Cassinello, Pilar Garcia-Alfonso, and Antonio Jimeno. 2009. Integration of panitumumab into the treatment of colorectal cancer. *Critical Reviews in Oncology/Hematology* .
- Grothey, Axel MD. 2006. Defining the role of panitumumab in colorectal cancer. *Community Oncology* 3:10–16.
- InfoNet, AIDS. 2009. Normal laboratory values. URL <http://www.aids.org/factSheets/120-Normal-Laboratory-Values.html>.
- Janeway, C.A., P. Travers, Jr, M. Walport, and M.J. Sclomchik. 2005. *Immunobiology*. Garland Science Publishing.
- Johnston, Matthew, Carina Edwards, Walter Bodmer, Philip Maini, and Jonathan Chapman. 2007. Mathematical modeling of cell population dynamics in the colonic crypt and in colorectal cancer. *PNAS* 104:4008–4013.
- Kurai, Jun, Hiroki Chikumi, Kiyoshi Hashimoto, Kosuke Yamaguchi, Akira Yamasaki, Takanori Sako, Hirokazu Touge, Haruhiko Makino, Miyako Takata, Masanori Miyata, Masaki Nakamoto, Naoto Burioka, and Eiji Shimizu. 2007. Antibody-dependent cellular cytotoxicity mediated by cetuximab against lung cancer cell lines. *Clin Cancer Res* 13:1552–1561.
- Kuznetsov, Vladimir, Iliya Makalkin, Mark Taylor, and Alan Perelson. 1994. Nonlinear dynamics of immunogenic tumors: Parameter estimation and global bifurcation analysis. *Bulletin of Mathematical Biology* 56:295–321.
- Lee, Peter P., Cassian Yee, Peter A. Savage, Lawrence Fong, Dirk Brockstedt, Jeffrey S. Weber, Denise Johnson, Susan Swetter, John Thompson, Philip D. Greenberg, Mario Roederer, and Mark M. Davis. 1999. Characterization of circulating T cells specific for tumor-associated antigens in melanoma patients. *Nat Med* 5:677–685.

Leith, John, Seth Michelson, Lynn Faulkner, and Sarah Bliven. 1987. Growth properties of artificial heterogeneous human colon tumors. *Cancer Research* 47:1045–1051.

Lenz, Heinz-Josef. 2007. Cetuximab in the management of colorectal cancer. *Biologics: Targets & Therapy* 2:77–91.

Lewis, James MD. 2009. Water and sodium balance: Fluid and electrolyte metabolism: Merck manual professional. URL <http://www.merck.com/mmpe/sec12/ch156/ch156b.html>.

Martinelli, E., R. De Palma, M. Orditura, F. De Vita, and F. Ciardiello. 2009. Anti-epidermal growth factor receptor monoclonal antibodies in cancer therapy. *Clinical and Experimental Immunology* 158:1–9.

Meropol, N.J., G.M. Barresi, T.A. Fehniger, J. Hitt, M. Franklin, and M.A. Caligiuri. 1998. Evaluation of natural killer cell expansion and activation in vivo with daily subcutaneous low-dose interleukin-2 plus periodic intermediate-dose pulsing. *Cancer Immunol Immunother* 46:318–326.

National Cancer Institute. 2010. Dictionary of cancer terms. URL <http://www.cancer.gov/dictionary/>.

Noble, Charles O., Michal T. Krauze, Daryl C. Drummond, Yoji Yamashita, Ryuta Saito, Mitchel S. Berger, Dmitri B. Kirpotin, Krystof S. Bankiewicz, and John W. Park. 2006. Novel nanoliposomal cpt-11 infused by convection-enhanced delivery in intracranial tumors: Pharmacology and efficacy. *Cancer Res* 66:2801–6.

Novartis Pharmaceuticals. 2007. Proleukin (aldesleukin): Pharmacology and indications. URL <http://www.proleukin.com/hcp/tools/pi-pharmacology.jsp>.

Orditura, M., C. Romano, F. De Vita, G. Galizia, E. Lieto, S. Infusino, G. De Cataldis, and G. Catalano. 2000. Behavior of interleukin-2 serum levels in advanced non-small-cell lung cancer patients: Relationship with response to therapy and survival. *Cancer Immunol Immunother* 49:530–536.

Pittet, Mikaël J., Danila Valmori, P. Rod Dunbar, Daniel E. Speiser, Danielle Liénard, Ferdy Lejeune, Katharina Fleischhauer, Vincenzo Cerundolo, Jean-Charles Cerottini, and Pedro Romero. 1999. High frequencies of naïve melan-a/MART-1-specific CD8+T cells in a large proportion of human histocompatibility leukocyte antigen (HLA)-A2 individuals. *J Exp Med* 190:705–715.

- Ratain, MJ. 1998. Body-surface area as a basis for dosing of anticancer agents: Science, myth, or habit? *J Clin Oncol* 16:2297–2298.
- Reya, Tannishtha, and Hans Clevers. 2005. Wnt signalling in stem cells and cancer. *Nature* 434:843–850.
- Rodriguez, Javier, Antonio Viudez, Mariano Ponz-Sarvisé, Isabel Gil-Aldea, Ana Chopitea, Jesus Garcia-Foncillas, and Ignacio Gil-Bazo. 2009. Improving disease control in advanced colorectal cancer: Panitumumab and cetuximab. *Critical Reviews in Oncology/Hematology* 1–9.
- Rosenberg, Steven. 1988. The development of new immunotherapies for the treatment of cancer using interleukin-2: A review. *Annals of Surgery* 208.
- RxList. 2009a. Erbitux drug information. URL <http://www.rxlist.com/erbitux-drug.htm>.
- . 2009b. Vectibix drug information. URL <http://www.rxlist.com/vectibix-drug.htm>.
- Siena, Salvatore, Andrea Sartore-Bianchi, Federica Di Nicolantonio, Julia Balfour, and Alberto Bardelli. 2009. Biomarkers predicting clinical outcome of epidermal growth factor receptor-targeted therapy in metastatic colorectal cancer. *Journal of the National Cancer Institute* 101:1–17.
- Sobrero, Alberto F., Joan Maurel, Louis Fehrenbacher, Werner Scheithauer, Yousif A. Abubakr, Manfred P. Lutz, M. Eugenia Vega-Villegas, Cathy Eng, Ernst U. Steinhauer, Jana Prausova, Heinz-Josef Lenz, Christophe Borg, Gary Middleton, Hendrik Kröning, Gabriele Luppi, Oliver Kisker, Angela Zobel, Christiane Langer, Justin Kopit, and Howard A Burris, III. 2008. EPIC: Phase III trial of cetuximab plus irinotecan after fluoropyrimidine and oxaliplatin failure in patients with metastatic colorectal cancer. *J Clin Oncol* 26:2311–2319.
- Sompayrac, Lauren. 2004. *How Cancer Works*. Jones and Bartlett Publishers.
- . 2008. *How the Immune System Works*. Blackwell Publishing.
- Speiser, Daniel E., Marco Colonna, Maha Ayyoub, Marina Cella, Mikaël J. Pittet, Pascal Batard, Danila Valmori, Philippe Guillaume, Danielle Liénard, Jean-Charles Cerottini, and Pedro Romero. 2001. The activatory

receptor 2b4 is expressed in vivo by human CD8 + effector  $\alpha\beta$ t cells. *J Immunol* 167:6165–6170.

Tsuruo, T., T. Matsuzaki, M. Matsushita, H. Saito, and T. Yokokura. 1988. Antitumor effect of CPT-11, a new derivative of camptothecin, against pleiotropic drug-resistant tumors in vitro and in vivo. *Cancer Chemo Pharm* 21:71–4.

Vilar, E., M. Scaltriti, J. Balmaña, C. Saura, M. Guzman, J. Arribas, J. Baselga, and J. Taberno. 2006. Defining the role of panitumumab in colorectal cancer. *Community Oncology* 3:10–16.

Voet, Donald, Judith Voet, and Charlotte W. Pratt. 2008. *Fundamentals of Biochemistry*. John Wiley & Sons, Inc., 3rd ed.

Welink, J., E. Boven, J.B. Vermorcken, H.E. Gall, and W.J. van der Vijgh. 1999. Pharmacokinetics and pharmacodynamics of lobaplatin (D-19466) in patients with advanced solid tumors, including patients with impaired renal or liver function. *Clin Cancer Res* 5:2349–58.